Linear precoding for multicarrier and multicast PLC

Jean-Yves Baudais, Matthieu Crussière

18. Linear precoding for multicarrier and multicast PLC

Jean-Yves Baudais and Matthieur Crussière

Contents of the chapter

1 Introduction

Since their introduction during 1960's as a solution to the issue of high-bit-rate transmission over dispersive communication channels, multicarrier techniques have intensively been studied and proposed in many communication standards [1]. Well-known under the acronym of OFDM, standing for orthogonal frequency division multiplexing, and first envisaged for wireless transmissions, multicarrier concepts have also been proposed for digital transmission over copper wire subscriber loop (DSL) systems under the digital multitone (DMT) terminology. For ten years, multicarrier schemes have become the basis of the physical layer of all modern communication standards, from European digital video broadcasting (DVB) to American IEEE-802.11 wireless local area network (WLAN) and worldwide 4G cellular systems. In the PLC landscape, multicarrier schemes have also been adopted by the HomePlug Alliance and integrated as the baseline technology for the HomePlug AV specification.

The reasons for such a success story come from its robustness in the case of frequency selective fading channels, its capability of portable and mobile reception and its flexibility. The multicarrier concept relies on the conversion of a serial high rate stream into several low rate streams distributed over closely spaced orthogonal sub-carriers or tones. Using a sufficiently large number of sub-carriers, any frequency selective channel can hence be converted into non-interfering flat fading sub-channels. As a result, single tap frequency based equalisation can be carried out to compensate for channel distortions instead of time-domain filter equalisation as needed in single carrier systems. Last but not least, multicarrier systems can be employed to realise a spectral efficiency benefit by adaptively sizing the data constellation used in each sub-carrier with respect to its SNR. This principle, referred to as adaptive loading, can be easily implemented in PLC systems since the SNR values can accurately be measured in the receiver and communicated to the transmitter over a feedback channel.

Apart from multicarrier schemes, spread spectrum is another communication strategy that takes on a significant role in cellular and personal communications [2]. The name spread spectrum stems from the fact that the transmitted signals occupy a much wider frequency band than is required to transmit the information. This confers many well-known advantages to spread spectrum signals such as immunity against multipath distortion, resistance to jamming, low power transmission possibility and signal hiding capability. Spread spectrum signals were originally designed by the military services to overcome either intentional or unintentional interference, but are today used to provide reliable communications in a variety of commercial applications. For example, spread spectrum signals are used in the so-called unlicensed frequency ISM bands at 2.4 GHz for cordless telephones, wireless LAN's and Bluetooth. But, more interestingly, spread spectrum signals can also provide communications to several concurrent users through code-division multiple access (CDMA) when using pseudo-random patterns. CDMA is employed in several wireless cellular standards such as IS-95, WCDMA and UMTS.

The advantages and success of multicarrier and spread spectrum techniques motivated many researchers to investigate the suitability at the combination of both techniques [3]. This combination known as multicarrier spread spectrum (MC-SS) benefits from the main advantages of both schemes: high spectral efficiency, high flexibility, multiple access capabilities, narrow-band interference rejection, simple one-tap equalisation, etc. MC-SS schemes can actually be viewed as an extension of the multicarrier concept in case the information data stream to be transmitted is linearly precoded using spreading sequences. Many variations around the MC-SS concept have been introduced during the 90's trying to find the most efficient precoding function to use along with the multicarrier modulation, essentially depending on the way this function is carried out: time-wise or frequency-wise, before or after multicarrier modulation, or even exploiting or not multiple access capabilities. Whereas this concept has been originally proposed for multicarrier access scheme, it can be extended to single user multicarrier systems and it is referred as linear precoded OFDM (LP-OFDM) [4]. As far as wire-line communications are concerned, MC-SS has been firstly proposed in [5, 6] for xDSL transmission and later for PLC [7, 8], hereby demonstrating the interest of the precoding concept in terms of bit-rate maximisation.

In this chapter we review the principles and the major results of the adaptive LP-OFDM communication system. Improvements encountered in adaptive multicarrier systems can in fact also be obtained in adaptive LP-OFDM systems. Therefore, the bit-rate maximisation problem is described and analysed in the power line communication context. Significant bit-rate gains are reached integrating a simple precoding function in the transmission scheme, and modifying conventional bit-loading algorithms in accordance with the waveform modification. To illustrate the benefit of the precoding concept, we propose to treat the problem of bit-rate maximisation under the simple target symbol error rate (SER) or noise margin constraint at first, and then under the more challenging constraint of target bit error rate (BER).

Also, to take fully advantage of the precoding function flexibility, we propose to optimise the LP-OFDM system using frequency, time and even 2D precoding. Point-to-point and multicast point-to-multipoint transmissions are simulated through in-home power line channels to quantify the bit-rate gains.

The chapter is organised as follows. The multicarrier system and the linear precoding function are introduced and described in Section 2. In this section, we also propose a synthetic study on resource allocation considering the case of discrete bit allocation. Then, Section 3 analyses the problem of resource allocation for bit-rate maximisation when discrete modulations are employed. A time-frequency application of the precoding is analysed in Section 4. The multicast context is investigated in Section 5 and numerical examples highlight the powerfulness of the linear precoding. Section 6 concludes the chapter.

2 Linear precoding for multicarrier systems

2.1 System model

As mentioned in the introduction, the reference model proposed herein is based on linearly precoded multicarrier modulation, referred to in the sequel as LP-OFDM. Let us first introduce the OFDM system and the related signal and then give the extension to LP-OFDM.

2.1.1 OFDM system

A simple representation of an OFDM system is given in Figure 1 where the precoding and deprecoding blocks have first to be ignored. In this model, basically, the binary information data stream enters a modulation and coding block which produces series of n digitally modulated symbols, such as quadrature amplitude modulations (QAM) mapped symbols for instance. Those n symbols are then multiplexed in the frequency domain by the OFDM function which ensures their parallel transmission onto n orthogonal sub-carriers. Assuming a convenient choice of the OFDM parameters with respect to the channel characteristics, and perfect time and frequency synchronisation of the receiver, the transmission system can essentially be modelled as n independent and non-interfering flat fading links or sub-channels in parallel associated to the n sub-carriers of the OFDM modulation. Hence, the input-output relationship of the ith sub-carrier can directly be written in the frequency domain as follows,

$$y_i = h_i s_i + v_i, \tag{1}$$

where $\{s_i\}_{i=1}^n$ and $\{y_i\}_{i=1}^n$ are the transmitted and received symbols in sub-carrier i respectively, $\{v_i\}_{i=1}^n$ are related to white Gaussian noise samples with variance σ^2, and $\{h_i\}_{i=1}^n$ are the complex channel coefficients modelling the amplitude and phase rotations independently experienced by the symbols in each sub-carrier i.

The PLC channel varies in time with long-term and short-time variations [9]. This time varying nature requires periodic estimation of the channel to perform equalisation or channel adaptation [10]. The channel can be considered quasi-static between two estimations and it is possible to integrate resource allocation functionalities at the transmitter side as depicted in the system model. This means that the OFDM transmitter will have the opportunity to adapt the order of the symbols of each sub-carrier and to allocate an appropriate amount of power to these symbols according to the known channel gain. Following this idea, the transmitted symbols are written as

$$s_i = \sqrt{p_i} x_i, \tag{2}$$

where symbols x_i are assumed to be unit-power whatever the order of the selected constellations, i.e. $E[x_i x_i^*] = 1$, $\forall i$, and power scaling factors p_i are supposed to be obtained through a power allocation policy as it will be detailed in Section 3. Throughout the chapter, $(\cdot)^*$ will stand for conjugate transpose which reduces to conjugate for scalar and transpose for real matrix.

Using matrix representations finally leads to the following expression

$$Y = HP^{1/2}X + N, \tag{3}$$

where Y, X and N are column vectors of length n with elements y_i, x_i and v_i respectively, and H and P are diagonal matrices of size $n \times n$ filled up with the h_i and the p_i respectively.
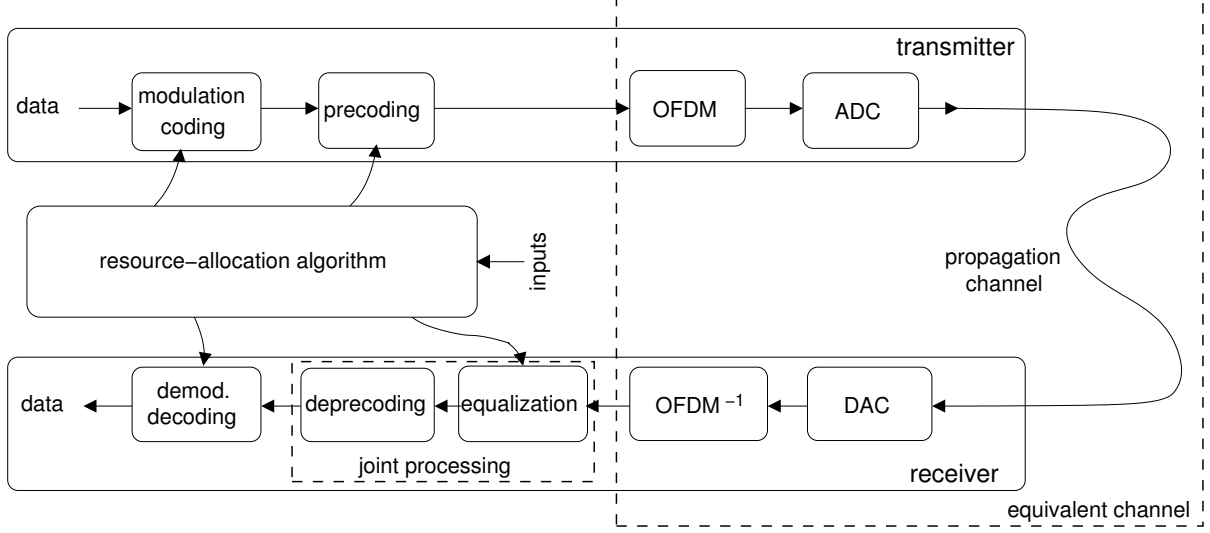
Figure 1: LP-OFDM communication system.

Assuming that the channel state information (CSI) is made available at the receiver owing to a channel estimation function, channel gain h_i can easily be compensated for through a linear detector consisting in a one tap equalisation per sub-carrier. This leads to the following estimated symbols Z

$$Z = WY = WHP^{1/2}X + WN,$$ (4)

where W is the equalisation matrix whose elements can be derived from various equalisation criteria as for instance zero forcing (ZF) or mean square error (MSE). In OFDM, all these criteria lead to equivalent system performance and W is usually chosen as

$$W = (H^*H)^{-1}H^*,$$ (5)

which is simply reduced to H^{-1}.

2.1.2 LP-OFDM system

The LP-OFDM system is simply obtained activating the precoding and deprecoding functions in the generic system model in Figure 1. Consequently, note that the resource allocation algorithm has to take into consideration the waveform structure modification. This aspect will be fully investigated in Section 3 in the case of system throughput maximisation.

As discussed in the introduction, many variations of the precoding function can be proposed, depending on which dimension (namely time, frequency or both) it is applied to. Considering PLC applications, time precoding is proposed in [11] as in the well known MC-DS-CDMA waveform, frequency precoding is studied in [12] leading to the so-called MC-CDMA waveform, and extension to 2D precoding is investigated in [13]. For the sake of clarity, we give a complete and comprehensive study in the case of frequency domain precoding in this part and further considerations about time and 2D precoding will be given in Section 4.

Considering frequency domain precoding, the mathematical expression of the OFDM signal has to be updated to yield that of the LP-OFDM signal. This is achieved by means of a precoding matrix denoted $C \in \mathbb{R}^{n \times n}$ which is applied to symbol vector S defined in (2). The received signal then writes

$$Y = HCP^{1/2}X + N.$$ (6)

Matrix C contains the precoding sequences that realise the spreading of the set of symbols X over the n sub-channels defined by the multicarrier system structure. Many solutions can be envisaged to build or give a particular structure to the precoding matrix C as detailed in the following section. Note that simply choosing $C = I_n$, with I_n being the identity matrix of size $n \times n$, amounts, in fact, to the traditional OFDM system.

As in the OFDM case, linear detectors can be used at the receiver to deal with the channel distortions. However, the frequency selectivity of the propagation channel destroys the precoding structure embedded in the LP-OFDM signal, which translates into interference between the precoded symbols called mutual code interference (MCI). Hence, the detector performance strongly depends on its capability to handle the MCI while mitigating the Gaussian noise effect. For instance, an MRC detector yields poor performance in LP-OFDM [14], whereas ZF and MMSE detectors are worth of interest. The ZF criteria leads to the following general expression of the detector [15]

$$W_{\mathrm{ZF}} = \left(P^{1/2} C^* H^* H C P^{1/2} \right)^{-1} P^{1/2} C^* H^*, \tag{7}$$

where the equalisation and the precoding are jointly treated. Such a detector perfectly compensates for the MCI and is able to extract the information symbols x_i without any interference. It can then be viewed as a decorrelating detector but however leads to a significant noise term boost. On the other hand, the MMSE detector writes

$$W_{\mathrm{MMSE}} = \left(P^{1/2} C^* H^* H C P^{1/2} + \sigma^2 I_n \right)^{-1} P^{1/2} C^* H^*. \tag{8}$$

The MMSE detector is the optimal linear detector since it trades off MCI reduction against noise effect mitigation. However, its complexity turns out to be much higher than that of the ZF detector. In the sequel, we will analyse in what extend the use of the ZF or the MMSE detector has impact on the resource allocation efficiency.

2.2 Optimum linear precoding

A first step in the LP-OFDM system design and resource allocation optimisation is to lead investigations about the kind of precoding sequences that should be used in the system. The optimal choice can be found by computing the constraint mutual information between the transmitted and received LP-OFDM signals as a function of matrix C. Assuming information vectors X and Y defined earlier as Gaussian vectors, and exploiting the multicarrier waveform structure of the LP-OFDM signal as n non-interfering Gaussian links, we have [12]

$$I(X|H,Y|H) = \log_2 \det \left(I_n + \frac{1}{\sigma^2} H C R_S C^* H^* \right), \tag{9}$$

where $R_S = \mathrm{E}\left[SS^* \right]$ represents the data symbol covariance matrix of size $n \times n$. From previous definition of S, R_S is then a diagonal matrix with diagonal elements $\{p_i\}_{i=1}^n$, which yields

$$I(X|H,Y|H) = \log_2 \det \left(\underbrace{I_n + \frac{1}{\sigma^2} H C P C^* H^*}_{A} \right). \tag{10}$$

Then, using Hadamard inequality [16] to find an upper bound to the determinant of matrix A, it comes

$$|\det(A)| \leq \prod_{i=1}^n ||A_i||_2, \tag{11}$$

with A_i the ith column of matrix A, and $||.||_2$ the Euclidean norm. This determinant is maximised if and only if vectors A_i are mutually orthogonal, i.e. $\forall i \neq j \; A_i^* A_j = 0$. Leading the calculation gives the following equation

$$A_i^* A_j = \frac{2}{\sigma^2} \Re \left(h_i h_j^* \right) C_i^T P C_j + \frac{1}{\sigma^2} h_i h_j^* \sum_{l=1}^n C_l^* P C_i |h_i|^2 C_j^* P C_l, \tag{12}$$

from which it can be noticed that imposing P to be an identity matrix, and C_i, C_j to be orthogonal sequences for all $i \neq j$, are sufficient conditions to have $A_i^* A_j = 0$. This is simply obtained choosing C as a Hadamard matrix

while assigning the same amount of power to each code sequence C_i, i.e. having $p_i = p$ for all $i \in [1,n]$. Note that there exist some other sequences, not necessarily orthogonal, that also lead to maximal constraint mutual information. Nevertheless, the proposed overview focuses on orthogonal sequences. To give more generality and flexibility to the precoding process, we however use the set $\mathscr{C}$ of orthogonal matrices which are composed of Hadamard matrices with the following definition.

Definition 1. *Let $\mathscr{C}$ be the set of optimal precoding matrices such that*

$$C \in \mathscr{C} \Longleftrightarrow c_{i,j} \in \{-1,0,1\} \ \text{and} \ C_i^T C_j = 0, \ \forall i \neq j.$$

Following this definition, the precoding matrix can be sparse. The data symbols that are precoded by C, are consequently not necessarily spread all over the multicarrier spectrum but can be rather limited to a subset of sub-carrier. The corresponding system can then be view as a multiple block system as proposed in [17]. This idea can be exemplified by the following sparse precoding matrix

$$C = \begin{pmatrix} 1 & 1 & 1 & 1 & 0 & 0 \\ 1 & -1 & 1 & -1 & 0 & 0 \\ 0 & 0 & 0 & 0 & 1 & 1 \\ 1 & 1 & -1 & -1 & 0 & 0 \\ 0 & 0 & 0 & 0 & 1 & -1 \\ 1 & -1 & -1 & 1 & 0 & 0 \end{pmatrix}. \tag{13}$$

This matrix is orthogonal and exhibits two precoding blocks: the first block, corresponding to the first four columns, spreads four data symbols across four sub-carriers, and the second block, related to the last two columns, spreads two data symbols across two other sub-carriers.

When the precoding matrix is not sparse, C is then reduced to a classical Hadamard matrix of order n, as stated by the following property.

Property 1. *If $\exists i$ such as $||C_i||_2^2 = n$ then $||C_j||_2^2 = n$ for all $j \in [1,n]$ and C is an Hadamard matrix with $n \in \{1,2,4s|s \in \mathbb{N}\}$ and $CC^T = nI_n$.*

The Hadamard conjecture proposes that Hadamard matrices exist for sizes n with $n = 1$, $n = 2$ or n being a multiple of 4. Hence, the well-known Sylvester method [18], which gives a simple solution for the construction of Hadamard matrices of size $n = 2^s$, is not sufficient to build all possible Hadamard matrices. Paley, Turyn or Williamson methods [18] help to find other sizes of matrices. For example, for $n = 12$, the Hadamard matrix can be

$$C = \begin{pmatrix} +1 & -1 & -1 & -1 & -1 & -1 & -1 & -1 & -1 & -1 & -1 & -1 \\ +1 & +1 & -1 & +1 & -1 & -1 & -1 & +1 & +1 & +1 & -1 & +1 \\ +1 & +1 & +1 & -1 & +1 & -1 & -1 & -1 & +1 & +1 & +1 & -1 \\ +1 & -1 & +1 & +1 & -1 & +1 & -1 & -1 & -1 & +1 & +1 & +1 \\ +1 & +1 & -1 & +1 & +1 & -1 & +1 & -1 & -1 & -1 & +1 & +1 \\ +1 & +1 & +1 & -1 & +1 & +1 & -1 & +1 & -1 & -1 & -1 & +1 \\ +1 & +1 & +1 & +1 & -1 & +1 & +1 & -1 & +1 & -1 & -1 & -1 \\ +1 & -1 & +1 & +1 & +1 & -1 & +1 & +1 & -1 & +1 & -1 & -1 \\ +1 & -1 & -1 & +1 & +1 & +1 & -1 & +1 & +1 & -1 & +1 & -1 \\ +1 & -1 & -1 & -1 & +1 & +1 & +1 & -1 & +1 & +1 & -1 & +1 \\ +1 & +1 & -1 & -1 & -1 & +1 & +1 & +1 & -1 & +1 & +1 & -1 \\ +1 & -1 & +1 & -1 & -1 & -1 & +1 & +1 & +1 & -1 & +1 & +1 \end{pmatrix}. \tag{14}$$

For $n > 12$ there exist multiple distinct Hadamard matrices. The first order of unknown Hadamard matrix is 668 and, up to now, only 13 matrices of size lower than 2000 are not known. In the sequel and for the theoretical analysis, we will admit that all sizes of Hadamard matrices are available. In practical systems, there are enough Hadamard matrices to design the precoded systems.

2.3 Power line constraints and bit-rate maximisation problem formulation

In the perspective of resource allocation optimisation, let us remind the constraints encountered in the power line context [19].

2.3.1 *Power spectrum mask*

The first constraint is the power spectrum mask that limits the transmitted power for each sub-carrier of the OFDM signal. Consequently, PLC transmissions have to fulfil peak-power rather than sum-power conditions. With a power upper limit of p on each sub-carrier, we can derive the peak-power constraint for an OFDM signal as follows,

$$E\left[||P^{1/2}X||_\infty^2\right] \le p. \tag{15}$$

Using (2), it yields

$$p_i \le p \; \forall i \in [1;n]. \tag{16}$$

Now considering the LP-OFDM system, the precoding matrix C is added in (15) and the peak-power constraint writes

$$E\left[||CP^{1/2}X||_\infty^2\right] \le p, \tag{17}$$

which leads to

$$\sum_{i=1}^{n} p_i \le p \tag{18}$$

for non sparse precoding matrices. With uniform power allocation this constraint leads to $p_i \le p/n$ for all i. Interestingly, from this equation, we can notice that the precoding function brings about the following property.

Property 2. *Orthogonal precoding converts the peak-power constraint into a sum-power constraint.*

The precoding, in fact, introduces some dependency between the data symbols at the transmitter side that transforms the peak constraint to sum constraint. Contrary to peak constraint, the sum constraint permits flexibility in allocation to fully exploit the power constraint p with multiple choices for the p_i.

Taking into account that many notches are specified in the PLC power mask, the effective peak power constraint can not be considered as uniform over the whole bandwidth. This can however be translated into a uniform peak-power constraint by integrating the power mask fluctuations into the channel transfer function, i.e. defining new channel coefficients $h_i' = \alpha_i \cdot h_i$, where α_i correspond to weighting factors depending on the power mask. More importantly, for LP-OFDM, the set $\mathscr{C}$ in Definition 1 remains optimal even under non uniform peak-power constraint. From these perspectives, the power mask will be considered as flat in the following without loss of generality.

2.3.2 *Constellations of discrete orders*

The second constraint is the discrete nature of the constellation size. The number r_i of bits per constellation symbol is the bit-rate per two-dimensional symbol and is defined in the set $\{0, \beta, 2\beta, 3\beta, \cdots, r_{\max}\}$ with $\beta > 0$. The maximal constellation size is given by $r_{\max}$ and the granularity of the constellations is given by β which has the same unit as r_i. This has strong impact in practice when peak-power constraint is considered since the constellation size can not be finely adjusted to the available amount of peak-power p when the number of possible sizes is limited. In other words, the peak-power constraint imposes to use β as low as possible to reduce the bit-rate loss due to the under-exploitation of the peak-power. Considering the modulation and the channel coding as a couple, it is possible to define β lower than 1. At the contrary, without any channel coding, $\beta = 1$ for all sizes of square and rectangular QAM. In practice, the ultimate measure is the coded error rate of the communication system. However, the coded error rate is strongly related to the uncoded one and the channel coding and modulation designs are separable issues [20, 21]. Therefore, we focus on the uncoded part of the system to design it in the following and we will assume β integer.

2.3.3 Target SNR-gap and BER

The last constraint to consider is the quality of service (QoS). We propose to consider best effort applications, which means that the system has to operate at maximum bit-rate. The QoS turns into a constraint of maximum target error rate from the physical layer point of view. In practice, a so-called SNR-gap is usually introduced to give some confidence to the target error rate [22]. The SNR-gap, or power-gap, is a convenient mechanism for analysing systems that transmit below channel capacity, or constraint capacity, or without Gaussian input, and the bit-rate becomes

$$r_i = \log_2 \left(1 + \frac{\mathsf{snr}_i}{\gamma_i} \right). \tag{19}$$

This gap γ_i depends on the constellation, coding format and error probability. The QAM approximation leads to $\gamma_i = \gamma$ independent of i under SER constraint [22]. With BER constraints, the QAM approximation is less accurate and using γ_i instead of γ [23] leads to higher bit-rate. We consider both SER and BER constraints to design LP-OFDM systems. The results are mainly developed with SER constraint and the BER constraint is treated as an extension.

2.3.4 Problem formulation

Eventually, the optimisation of the proposed PLC system consists in the maximisation of the bit-rate taking into account the above mentioned constraints. This can be summarised in the form of the following problem.

Problem 1. *Maximise the bit-rate under peak-power constraint p per carrier, under discrete and finite number of bits or bit-rate r_i per two dimensional symbol, $r_i \in \{0, \beta, 2\beta, 3\beta, \cdots, r_{\max}\}$, under error rate or noise margin constraint, and with precoding matrices defined in $\mathscr{C}$.*

2.4 Continuous bit-rate considerations

Before solving the above stated problem, it is interesting to lead analysis relaxing the constraint of discrete constellations. Hereby, we enable the use of continuous bit-rate in the system, i.e. $r_i \in \mathbb{R}_+$. It is then possible to make use of convex optimisation tools and analytically find the optimal set of power allocation $\{p_i\}_{i=1}^n$ to be used in the LP-OFDM system to maximise the total bit-rate. The results are developed hereafter and will be used as benchmark for the constrained discrete case in the next section.

For the sake of clarity and without loss of generality, the analysis of the problem is firstly presented assuming non sparse precoding matrix C, with C of Hadamard type. We focus on linear receivers as previously mentioned in (7) and (8) where the matrix W of the detector jointly realises the equalisation and deprecoding process. Two receivers are analysed: the decorrelating detector and the optimal linear detector. The predistortion is also considered in the case of ZF criterion. As the precoding is used at transmitter side to improve the bit-rate, we may ask whether the channel can be also corrected at the transmitter side, i.e. using predistortion. The predistortion is then compared to the equalisation with ZF criterion before analysing the optimal linear detector.

2.4.1 Decorrelating detector

The general expression of the detector matrix is given in (7). In our case, with invertible and square matrices, the matrix of the detector reduces to

$$W = \frac{1}{n} P^{-1/2} C^T H^{-1}, \tag{20}$$

which yields

$$Z = X + \frac{1}{n} P^{-1/2} C^T H^{-1} N. \tag{21}$$

Using this formulation, the equalisation and the deprecoding functions turn out to be separable as mentioned in Figure 1. Estimated symbols Z then writes as the transmitted ones, namely X, corrupted by a coloured noise term. The

total continuous bit-rate achieved by the system can consequently be viewed as the sum of the bit-rates $\{r_i\}_{i=1}^n$

$$R = \sum_{i=1}^n \log_2 \left(1 + \frac{1}{\gamma} \frac{n^2}{\sum_{j=1}^n \frac{1}{|h_j|^2}} \frac{p_i}{\sigma^2} \right). \tag{22}$$

Note that taking $\gamma = 1$ in this equation yields the system capacity, whereas R means the achievable bit rate at a given SER for $\gamma > 1$. It is then possible to state the bit-rate maximisation problem in the case of continuous bit-rates as follows.

Problem 2. *Maximise achievable bit-rate of the system* $\max\limits_{\{p_i,\ i\in[1,n]\}} R$ *under the power constraint* $\sum\limits_{i=1}^n p_i \leq p$, *with R given in* (22).

In this problem, the power constraint is stated as a sum constraint as explained earlier in the case of Hadamard precoding matrices (see Property 2). Since the term depending on the channel state in (22), namely $\sum_{j=1}^n |h_j|^{-2}$, does not depend on index i, it is straightforward to prove that the total achievable bit-rate writes [7]

$$R \leq n \log_2 \left(1 + \frac{1}{\gamma} \frac{n}{\sum_{j=1}^n \frac{1}{|h_j|^2}} \frac{p}{\sigma^2} \right). \tag{23}$$

This indicates that the optimal power allocation is obtained with $p_i = p/n$, $\forall i$ and the optimal bit allocation with R/n bits per precoding sequence. Interestingly, this result corroborates the previous analysis made in Section 2.2 concerning optimal precoding matrices. From there, we can state the following proposition which will be used as a reference result throughout the chapter.

Proposition 1. *The maximal achievable continuous bit-rate of an LP-OFDM system equipped with a ZF receiver and using Hadamard precoding matrices is reached with equal power and bit allocations under sum power constraint.*

Let us now analyse the impact of the precoding factor n on the maximum bit-rate, and particularly compare two cases: OFDM and LP-OFDM. In the case of continuous bit-rates, it can be seen that

$$n \log_2 \left(1 + \frac{1}{\gamma} \frac{n}{\sum_{j=1}^n \frac{1}{|h_j|^2}} \frac{p}{\sigma^2} \right) \leq \sum_{i=1}^n \log_2 \left(1 + \frac{1}{\gamma} \frac{|h_i|^2 p}{\sigma^2} \right), \tag{24}$$

equality being obtained if and only if $|h_i|$ is constant for all i. This means that the continuous bit-rate of precoded systems is lower than that of unprecoded ones as soon as frequency selectivity is experienced by the transmitted signal. In other words, the OFDM system provides the highest achievable throughput in that case. To go further, using the fact that the harmonic mean of an exponential distribution is zero and assuming $|h_i|$ are iid Rayleigh fading channel coefficients, it comes that the continuous bit-rate of an LP-OFDM system is upper-bounded by zero when the size of the precoding matrix tends to infinity. This very negative conclusion can be understood by the fact that the LP-OFDM system suffers from the noise boost induced by the ZF detector which effect is all the more destructive when the channel frequency selectivity is high.

2.4.2 Predistortion versus equalisation

Assuming CSI knowledge at the transmitter and under sum power constraint, it is well known that optimal power allocation is obtained through the water-filling algorithm [24]. Water-filling can in fact be viewed as a predistortion of the transmitted signal. With peak-power constraint however, previous results show that full power allocation per sub-carrier is the optimal allocation strategy for OFDM signalling. This eventually indicates that predistortion is not recommended in that case. Nevertheless, since we have shown that peak power constraint is converted to a sum power constraint when precoding is activated, it is interesting to raise the question whether it is useful to carry out predistortion with LP-OFDM. In the following, the question is addressed in the case of the ZF criterion.

Let W be the predistortion matrix instead of the equalisation matrix. With LP-OFDM, we then have

$$Z = \frac{1}{n}P^{-1/2}C^T\left(HWCP^{1/2}X + N\right). \tag{25}$$

Applying the ZF criterion at the transmitter side means that only the most attenuated sub-carrier is assigned the maximum peak power p. The other sub-carriers are attenuated such that the predistortion matrix is proportional to H^{-1}. This reads

$$W = H^{-1} \times ||H||_{-\infty}. \tag{26}$$

Clearly, the disadvantage of this approach is that the available power is largely under-exploited at the transmitter. To mitigate this, the correction of the channel can be shared between the transmitter and the receiver applying the conventional square root function. In a more general approach, the correction is performed using W^α at the transmitter and $W^{1-\alpha}$ at the receiver guaranteeing a total correction of W, with $\alpha \in [0,1]$. The continuous bit-rate is then

$$R = \sum_{i=1}^{n} \log_2\left(1 + \frac{n^2 \max_{j\in[1,n]} |h_j|^{2\alpha}}{\sum_{j=1}^{n} \frac{1}{|h_j|^{2(1-\alpha)}}} \frac{p_i}{\sigma^2}\right). \tag{27}$$

Note that the full predistortion is obtained with $\alpha = 1$, full equalisation with $\alpha = 0$, and uniform sharing is obtained with square-root $\alpha = 1/2$. The study of the function $f(\alpha) : \alpha \mapsto R$ actually shows that it is a decreasing function with maximal value achieved at $\alpha = 0$. Hence, the optimal strategy is to exploit all the available power and to treat the distortion introduced by the channel at the receiver side. This can be understood by the fact that predistortion always leads to transmit power reduction, and thus, bit-rate limitation. We can then state the following proposition.

Proposition 2. *Considering a precoded multicarrier system and with respect to the ZF criterion, the continuous and discrete bit-rates are higher with equalisation than with predistortion.*

Predistortion will then not be further investigated in the rest of the chapter.

2.4.3 Optimum linear detector

We may wonder whether conclusions drawn above in the ZF detector case would hold using the optimal MMSE linear detector. As such a detector has prohibitive complexity for practical implementations, simpler receivers have been proposed in the literature of wireless communications [14, 25] applying the MSE criterion sub-carrier per sub-carrier. This yields

$$W = \frac{1}{n}P^{-1/2}C^T\left(HPH^* + \sigma^2 I_n\right)^{-1}H^*. \tag{28}$$

The resulting detected symbols Z consist of a useful term, an MCI term and a noise term. They all depend on channel coefficients h_i, power allocation p_i and noise variance σ^2. Assuming that the MCI is an additional noise component, the total continuous bit-rate can be expressed after some mathematical manipulations as the sum of the bit-rates over dimension i [26],

$$R = \sum_{i=1}^{n} \log_2\left(1 + \frac{1}{\gamma}\frac{\mathrm{Tr}\left(HH^*(HH^* + \lambda I_n)^{-1}\right)^2 p_i}{\sum_{\substack{j=1 \\ j\neq i}}^{n}\left(C_i^T HH^*(HH^* + \lambda I_n)^{-1}C_j\right)^2 p_j + \mathrm{Tr}\left(HH^*(HH^* + \lambda I_n)^{-2}\right)\sigma^2}\right), \tag{29}$$

with

$$\lambda = \frac{\sigma^2}{\sum_{i=1}^{n} p_i}. \tag{30}$$

It can first be shown in that case that the continuous bit-rate obtained from (29) is the same as that computed in the general case using (8). However, whereas (8) needs to merge deprecoding and channel equalisation functions, (29) allows compatible architecture with conventional OFDM equalisation in which the receiver equalises the channel sub-carrier per sub-carrier and then deprecodes.

When the number of dimensions goes to infinity, i.e. $n \to \infty$, and using the fact that half of the terms in $C_i^T C_j$ are equal to 1 and half equal to -1, the asymptotic limit of (29) reduces to

$$\lim_{n\to\infty} \sum_{i=1}^{n} \log_2 \left(1 + \frac{1}{\gamma \log 2} \frac{\mathrm{E}\left[\frac{|h_i|^2}{|h_i|^2+\lambda}\right]^2 p_i}{\frac{n-1}{n}\left(\mathrm{E}\left[\left(\frac{|h_i|^2}{|h_i|^2+\lambda}\right)^2\right] - \mathrm{E}\left[\frac{|h_i|^2}{|h_i|^2+\lambda}\right]^2\right)(1-p_i) + \mathrm{E}\left[\frac{|h_i|^2}{(|h_i|^2+\lambda)^2}\right]\sigma^2} \right). \tag{31}$$

The sum over i depends only on p_i and it is independent on other power p_j. The power allocation that maximises the bit-rate is then the uniform one, as in the ZF case and as expected from Section 2.2. Hence we can let $p_i = p/n$ for all i and

$$\max_{\{p_i\}_{i\in[1,n]}} \lim_{n\to\infty} R = \frac{1}{\gamma \log 2} \frac{\mathrm{E}\left[\frac{|h_i|^2}{|h_i|^2+\lambda}\right]^2}{\mathrm{E}\left[\left(\frac{|h_i|^2}{|h_i|^2+\lambda}\right)^2\right] - \mathrm{E}\left[\frac{|h_i|^2}{|h_i|^2+\lambda}\right]^2 + \frac{\sigma^2}{p}\mathrm{E}\left[\frac{|h_i|^2}{(|h_i|^2+\lambda)^2}\right]}. \tag{32}$$

Contrary to the ZF receiver, the continuous bit-rate of MMSE receiver does not tend to zero but it remains lower than the OFDM continuous bit-rate. In high SNR regime it however tends to zero since the performance of the MMSE receiver tends to the performance of the ZF one. With a finite dimension n, the analysis is not tractable since the approximation no longer holds. Computing one simple case of two sub-carriers shows that with high channel distortions the bit-rate is maximised when total power is gathered on one single dimension, i.e. $p_1 = p$ and $p_2 = 0$, whereas with low channel distortions the uniform power allocation strategy maximises the bit-rate. In any case, the achievable continuous bit-rate remains lower in LP-OFDM than in OFDM. Note that with $\gamma = 1$, the continuous OFDM bit-rate is the channel capacity that can not be exceed by any linear and non linear receiver. The same conclusion is obtained with $\gamma > 1$ for both OFDM and LP-OFDM systems.

If we stopped the analysis at this step, we would conclude that the precoding function is not interesting and introduces substantial throughput loss compared to unprecoded systems. We will prove that conclusions can be far different in the case of discrete modulations. We will however keep in mind the main properties developed in these sections to better understand the system behaviour in the following.

3 Resource allocation for LP-OFDM

Let us now develop and give the solution to the resource allocation problem stated in Section 2.3.4 for LP-OFDM systems. In particular, we will show in what extent the precoding function provides additional flexibility to the bit and power allocation function and eventually leads to performance gain when adaptive modulations of finite order are employed.

Generally speaking, adaptive modulations allow to optimise the performance of a transmission scheme according to the link quality between the transmitter and the receiver. In multicarrier systems for instance, it provides the ability to assign different number of bits to different sub-carriers, hereby adapting the waveform parameters to the propagation conditions. By that means, different sub-carriers experiencing different channel gains can be assigned adequate number of bits and amount of power to finally achieve the same error rate. Many resource allocation algorithms designed for multicarrier systems can be found in the literature, with the aim of optimising either the bit-rate or the robustness of the system. The related problems are commonly referred to as *rate maximisation* problem and *margin maximisation* optimisation problem [27], respectively. However, as soon as a precoding function is integrated to the multicarrier system, as proposed herein, new resource allocation algorithms have to be derived, taking into account the waveform and system particularities. Indeed, additional parameters have to be adaptively computed, such as for instance the number or the length of the precoding sequences.

In this section, we propose to detail the key points of resource allocation mechanisms in LP-OFDM in comparison to more conventional OFDM systems. Perfect CSI will be assumed at the transmitter, which supposes perfect channel

estimation at the receiver and perfect information feedback to the transmitter. In practice however, perfect CSI is rarely achieved. The problem of imperfect CSI has already been discussed for OFDM systems and modified solutions for LP-OFDM systems can be found in [28, 29], where the bit-rate maximisation problem takes into account channel estimation inaccuracies.

3.1 Multicarrier system

To provide elements of comparison, let us first briefly derive the bit-rate maximisation algorithm under peak-power constraint for the OFDM system. Using (3) and (19), the highest achievable continuous bit-rate of an OFDM system under maximum peak-power p is

$$R = \sum_{i=1}^{n} \log_2 \left(1 + \frac{|h_i|^2 p}{\gamma \sigma^2} \right). \tag{33}$$

The discrete version r of this continuous bit-rate is then obtained as

$$r = \sum_{i=1}^{n} \lfloor r_i \rfloor_\beta = \sum_{i=1}^{n} \left\lfloor \log_2 \left(1 + \frac{|h_i|^2 p}{\gamma \sigma^2} \right) \right\rfloor_\beta, \tag{34}$$

with $\lfloor x \rfloor_\beta = \beta \lfloor x/\beta \rfloor_1$ and where $\lfloor \cdot \rfloor_1$ is the conventional floor operation. In this equation, $\lfloor r_i \rfloor_\beta$ denotes the discrete bit-rate achieved on sub-carrier i based on continuous bit-rate r_i. Accordingly, the effective power to assign to sub-carrier i to guarantee $\lfloor r_i \rfloor_\beta$ can be computed as

$$p_i = (2^{\lfloor r_i \rfloor_\beta} - 1) \frac{\gamma \sigma^2}{|h_i|^2} = p - \varepsilon_i, \tag{35}$$

where ε_i corresponds to the residual power available on sub-carrier i with respect to the peak-power limitation p. This amount of power is not sufficient to upgrade the constellation used on sub-carrier i with an additional bit. Hence, it is concluded that the floor operation limits the system capability of exploiting all the available power. This limitation can be evaluated using a so-called power efficiency factor. Let us define this power efficiency factor q_i for sub-carrier i as

$$q_i = 1 - \frac{\varepsilon_i}{p} = \frac{2^{\lfloor r_i \rfloor_\beta} - 1}{2^{r_i} - 1}. \tag{36}$$

Under the assumption of a uniform distribution of $r_i - \lfloor r_i \rfloor_\beta$ in $[0, \beta)$, the mean value of q_i is

$$m_{q_i} = \left(2^{\lfloor r_i \rfloor_\beta} - 1 \right) \left(\frac{1}{\beta} \log_2 \frac{2^{\lfloor r_i \rfloor_\beta + \beta} - 1}{2^{\lfloor r_i \rfloor_\beta} - 1} - 1 \right). \tag{37}$$

It can be computed that the mean power efficiency m_{q_i} remains lower than 72 % for all modulation orders, i.e. with $\beta = 1$, and lower than 54 % with $\beta = 2$. These figures indicate that there is room for system improvement through better power exploitation. This can be obtained choosing β as low as possible, which means using large varieties of modulation-coding couples. This however can lead to very complex receiver structures equipped with numerous channel decoders in parallel. Alternatively, we will show in the following section that linear precoding can provide better power efficiency factors with low complexity.

3.2 Linear precoding and multicarrier

It has be proven in Section 2.4 that the bit-rate maximisation for continuous rates leads to equal power allocation and then equal bit-rate per precoding sequence. As in the OFDM case, a simple allocation algorithm for discrete modulations would then consist in applying the floor operator to the continuous bit-rates derived from either (22) or (29). In that case, the uniform distribution of bits and power would be preserved. With discrete bit-rates, this is however shown as being suboptimal in the following.

3.2.1 Decorrelating detector

From Proposition 1, the maximal continuous bit-rate of a precoded system is

$$R = n\log_2\left(1 + \frac{1}{\gamma}\frac{n}{\sum\limits_{j=1}^{n}\frac{1}{|h_j|^2}}\frac{p}{\sigma^2}\right).$$ (38)

With discrete bit-rates, it can be proven that the maximal achievable bit-rate is computed according to the following proposition.

Proposition 3. *The maximal discrete bit-rate of an LP-OFDM system is [7]*

$$r = n\left\lfloor\frac{R}{n}\right\rfloor_\beta + \beta\left\lfloor n\frac{2^{R/n-\lfloor R/n\rfloor_\beta}-1}{2^\beta-1}\right\rfloor_1,$$

with R given by (38).

Comparing the results of this proposition to (34), we notice that, contrary to OFDM, it is possible in LP-OFDM to allocate a number of bits higher than that obtained through a simple floor operation applied to continuous bit-rates. In other terms, it becomes possible to improve the discrete bit-rate with precoding. Let us have a numerical example to simply illustrate this idea. Let us consider a flat fading channel, discrete modulations such that $\beta = 1$, and let the continuous bit-rate per sub-carrier be lower than 1 for all sub-carriers, i.e. $r_i = 1 - \varepsilon$ with $\varepsilon > 0$. The discrete bit-rate that would be achieved by the OFDM system without precoding would be zero. Now integrating a precoding function in the system, the continuous bit-rate given by (38) would become $R = n(1 - \varepsilon)$ and the discrete bit-rate given by Proposition 3 would be $r = \lfloor n(2^{1-\varepsilon} - 1)\rfloor$. For every ε, if n is large enough then the discrete bit-rate r can exceed one, which enables the transmission of at least one bit. (Note that in practice, n is limited by the maximum number of sub-carriers in the OFDM symbol.) Generalising this idea, it is understood that the precoding function has the capability to gather the pieces of power available on each sub-carrier of the multicarrier spectrum and consequently find resource to allocate additional bits compared to the non precoding case. In contrast to that, a conventional OFDM system exploits the power resource sub-carrier by sub-carrier without any gathering effect.

From Proposition 3, it is then possible to define the bit-rate allocation policy that yields the maximum discrete bit-rate for the LP-OFDM system. It is given by the following corollary.

Corollary 1. *The maximal discrete bit-rate is obtained with* $\left\lfloor n\frac{2^{R/n-\lfloor R/n\rfloor_\beta}-1}{2^\beta-1}\right\rfloor_1$ *precoding sequences carrying* $\lfloor R/n\rfloor_\beta + \beta$ *bits, and* $n - \left\lfloor n\frac{2^{R/n-\lfloor R/n\rfloor_\beta}-1}{2^\beta-1}\right\rfloor_1$ *precoding sequences carrying* $\lfloor R/n\rfloor_\beta$ *bits.*

Interestingly, the optimal allocation guarantees the lowest deviation of the bit-rate per dimension or per precoding sequence.

As in the OFDM system, the power efficiency of the precoded system is now evaluated. The useful power is the necessary and sufficient power to transmit the bit-rate given in Proposition 3. It then comes

$$\sum_{i=1}^{n}p_i = \left(2^{\lfloor R/n\rfloor_\beta}\left(n + (2^\beta - 1)\left\lfloor n\frac{2^{R/n-\lfloor R/n\rfloor_\beta}-1}{2^\beta-1}\right\rfloor_1\right) - n\right)\sum_{i=1}^{n}\frac{\gamma\sigma^2}{n^2|h_i|^2},$$ (39)

which leads to the following power efficiency factor

$$q = \frac{2^{\lfloor R/n\rfloor_\beta}\left(1 + \frac{2^\beta-1}{n}\left\lfloor n\frac{2^{R/n-\lfloor R/n\rfloor_\beta}-1}{2^\beta-1}\right\rfloor_1\right) - 1}{2^{R/n} - 1}$$ (40)

and we note that

$$\lim_{n\to\infty} q = 1.$$ (41)

$\lfloor R/n \rfloor$	$\beta = 1$			$\beta = 2$		
	$n = 1$	$n = 2$	$n = 16$	$n = 1$	$n = 2$	$n = 16$
1	0.58	0.75	0.96	0.40	0.60	0.93
2	0.67	0.81	0.97	0.48	0.66	0.94
5	0.72	0.84	0.98	0.53	0.70	0.95
10	0.72	0.84	0.98	0.54	0.70	0.95

Table 1: Mean power efficiency.

It finally appears that the precoding is all the more power efficient than the precoding matrix size increases. To illustrate this idea, Table 1 provides some numerical examples of power efficiency for $n \in \{1, 2, 16\}$. Note that the power efficiency factor q of an OFDM system is obtained with $n = 1$ in (40). Two values of β and four modulation orders are considered. The power efficiency clearly increases with the modulation order or the precoding sequence length, and decreases with β. Hence, the precoded system is unconditionally more efficient than the unprecoded one. The power efficiency even exceeds 90 % with n higher than 16.

We then conclude that the precoding matrix has to be large enough to make the power efficiency factor tend to 100%, or equivalently to make the discrete bit-rate achieve the maximal continuous one. At the same time however, as stated in Section 2.4, the continuous bit-rate goes to zero as the precoding matrix size increases due to channel frequency selectivity effects. We then understand that a trade-off has to be found on the precoding matrix size between the power efficiency increase and the frequency selectivity minimisation. As this will be exemplified in the following, the trade-off must be sought regarding channel conditions.

3.2.2 Optimum linear detector

Contrary to the decorrelating ZF receiver, there is no analytical solution for discrete bit-rate allocation with the MMSE receiver. The algorithmic approach is then investigated using an incremental allocation procedure. The basic idea is to iteratively load the precoding sequences with β bits, verifying at each iteration that the deviation of the discrete bit-rate allocation is minimised over the sequences. This is to obtain a bit-rate allocation as close as possible from the continuous bit-rate case. Obviously, the iterative allocation goes on as long as the power constraint is satisfied. To evaluate the power to be allocated to each additional β bit, let us define matrix $A = (a_{i,j})_{\{i,j\} \in [1,n]^2}$ such that

$$
\begin{cases}
a_{i,j} = (1 - 2^{r_i}) \left(C_i^T HH^* (HH^* + \lambda I_n)^{-1} C_j \right)^2, \ \forall i \neq j \\
a_{i,i} = \frac{1}{\gamma} \operatorname{Tr} \left(HH^* (HH^* + \lambda I_n)^{-1} \right)^2
\end{cases}
\tag{42}
$$

and diagonal matrix $B = (b_{i,j})_{\{i,j\} \in [1,n]^2}$ as

$$
b_{i,i} = (2^{r_i} - 1) \sigma^2 \operatorname{Tr} \left(HH^* (HH^* + \lambda I_n)^{-2} \right),
\tag{43}
$$

where we recall that r_i is the continuous bit-rate within the dimension i. Using (29) it is obtained that

$$
a_{i,i} p_i + \sum_{\substack{j=1 \\ j \neq i}}^{n} a_{i,j} p_j = b_i, \ \forall i \in [1, n].
\tag{44}
$$

Hence for a given set of bit-rate allocation $\{r_i\}_{i \in [1,n]}$ we can compactly write

$$
AP = B.
\tag{45}
$$

Finally, the convenient power allocation of an LP-OFDM system equipped with an MMSE detector has to respect the following proposition [26].

Proposition 4. *Assuming a bit-rate allocation $\{r_i\}_{i \in [1,n]}$, the power allocation that minimises the sum power is the diagonal matrix P such that $P = A^{-1}B$.*

To reduce the complexity of the algorithm and the number of iterations, Corollary 1 can advantageously be used to initialise the procedure. In other words, the bit and power allocation is realised in a first step as if the ZF detector were used. In a second step, the iterative procedure is launched and β bits are added iteratively sequence by sequence, each time re-computing the power allocation according to Proposition 4. Following this strategy, the discrete bit-rate achieved with the MMSE receiver is unconditionally higher or equal than that obtained with the ZF receiver.

3.3 BER constraint

As evident from the previous sections, resource allocation under SER constraint leads to simple optimisation strategies, since noise margin γ does not depend on the constellation order. In practical systems however, the QoS is often expressed in terms of BER, or packet error rate derived from BER, instead of SER. BER constraint is usually meant as average BER and several definitions can be given [30]. We define the mean BER constraint as

$$\frac{\sum\limits_{i=1}^{n} r_i \mathrm{ber}_i(r_i)}{\sum\limits_{i=1}^{n} r_i} \leq \mathrm{ber}, \tag{46}$$

where $\mathrm{ber}_i(r_i)$ is the BER within dimension i associated to r_i bits and ber is the target BER. Recall that dimension i corresponds to the ith sub-carrier of the OFDM system or the ith precoding sequence of the LP-OFDM one. One has to note that the BER resulting from streams of unequal bit-rates over i is not the arithmetic mean of individual BER per dimension but rather expresses as a weighted mean BER.

Unfortunately, this mean BER constraint leads to high computation time for optimal solution which is obtained with greedy-type algorithms. Basically, these algorithms iteratively allocate β bits at a time to the dimension that minimises the mean BER measure. Alternatively, suboptimal solutions can be sought considering peak BER rather than mean BER. In that case, the BER within each dimension is individually limited by the target BER. The constraint then reads

$$\mathrm{ber}_i(r_i) \leq \mathrm{ber}. \tag{47}$$

As introduced in (19), the BER constraint can be taken into account through the SNR-gap γ_i which depends on the constellation order, namely bit-rate r_i. Denoting $\gamma(r_i)$ this SNR-gap, it is possible to update Proposition 3 to give the optimal bit-rate allocation for LP-OFDM under target BER constraint. This is given by Proposition 5 below.

Proposition 5. *The maximal discrete bit-rate with precoding is [31]*

$$r = n \left\lfloor \frac{R}{n} \right\rfloor_\beta + \beta \left\lfloor n \frac{2^{R/n} - 2^{\lfloor R/n \rfloor_\beta}}{\left(2^{\lfloor R/n \rfloor_\beta + \beta} - 1 \right) \frac{\gamma\left(\lfloor R/n \rfloor_\beta + \beta\right)}{\gamma\left(\lfloor R/n \rfloor_\beta\right)} - 2^{\lfloor R/n \rfloor_\beta} + 1} \right\rfloor_1 = n \left\lfloor \frac{R}{n} \right\rfloor_\beta + \beta n',$$

with R given by (38) *and calculated with* $\gamma = \gamma(\lfloor R/n \rfloor_\beta)$.

Taking $\gamma(\lfloor R/n \rfloor_\beta) = \gamma(\lfloor R/n + \beta \rfloor_\beta) = \gamma$, that is for constant SNR-gap, Proposition 5 amounts to Proposition 3. Hence, Proposition 5 can be interpreted as a extension of Proposition 3 to the case where the SNR-gap is not constant. Interestingly, one can notice that the optimal bit allocation once again respects the already mentioned general principle which encourages a minimal bit-rate deviation over the dimension i. We can hence state the following Corollary.

Corollary 2. *The maximal discrete bit-rate is obtain with n' sequences carrying $\lfloor R/n \rfloor_\beta + \beta$ bits, and $n - n'$ sequences carrying $\lfloor R/n \rfloor_\beta$ bits.*

At high SNR asymptotic regime with square modulations and high modulation orders, it can be shown that the SER and BER constraints lead to equivalent performance [32], essentially owing to the fact that SER to BER translation can easily be obtained. At non asymptotic regime, it is difficult to convert SER to BER for the same operating point and the equivalence no more holds. In this case, performance comparison is irrelevant since the operating points differ.

n	1	2	5	10	20	50	100	1000
$q(n)$	1	2	31	28696	$1.64 \cdot 10^{12}$	$7.18 \cdot 10^{42}$	$1.80 \cdot 10^{106}$	$7.87 \cdot 10^{1835}$
$q'(n)$	1	2	4	14	71	1780	73486	$7.49 \cdot 10^{16}$
$q''(n)$	1	2	3	4	7	14	27	252

Table 2: Numbers of partitions.

3.4 Practical system design

In the previous sections, allocation procedures that maximise continuous and discrete bit-rates have been developed with non sparse precoding matrices, that is only considering Hadamard matrices of size n. To address the allocation problem, it remains yet to find the optimal matrix leading to a bit-rate maximisation within the set $\mathscr{C}$ given in Definition 1. As already mentioned in Section 2.2, such sparse matrices lead to multiblock precoded systems, each block corresponding to an Hadamard matrix of size lower than n. Allocation algorithms have then to find the optimal size for each precoding block and how to interleave them over the n sub-carriers. We already know that the optimal size of a non sparse precoding matrix should answer the trade-off between the increase of the power efficiency and the degradation of the system continuous bit-rate.

Unfortunately, there is no analytical solution to optimally design the sparse matrices. Indeed, the optimisation problem becomes a combinatorial optimisation problem that can be stated as: how to distribute n sub-carriers within subsets of size 1, 2 and all multiples of 4. The optimal solution is obtained through an exhaustive search over the number of partitions of a set with n elements and with constrained sizes of subsets. The generating function of such a number of partitions is

$$\exp\left(x + \frac{x^2}{2!} + \sum_{n=1}^{\infty} \frac{x^{4n}}{4n!}\right) = 1 + x + x^2 + \frac{2}{3}x^3 + \frac{11}{4!}x^4 + \cdots = \sum_{n=1}^{\infty} q(n)\frac{x^n}{n!}, \tag{48}$$

where $q(n)$ is the number of the partitions. Table 2 summarises some figures obtained with various values of n. It clearly appears that the problem becomes rapidly intractable for practical numbers of sub-carriers.

To reduce the number of combinations, it is valuable to split the problem into two sub-problems. Let M be the matrix such that $C = \Pi M$ with Π a permutation matrix, and

$$M = \begin{bmatrix} M_1 & & 0 \\ & \ddots & \\ 0 & & M_k \end{bmatrix}, \tag{49}$$

with $(M_l)_{l \in [1,k]}$ be the Hadamard matrices of size $n_l \times n_l$ that verifies

$$\sum_{l=1}^{k} n_l = n. \tag{50}$$

The problem then translates into the search of the k precoding matrices M_l on one hand, and the search of the permutation matrix Π on the other hand. Analytical solution is obtained for the design of matrix Π as stated below [7].

Proposition 6. *For a given matrix M, the permutation matrix Π that maximises the continuous bit-rate is such that: if M_l is distributed over the set of sub-carriers $\mathscr{H}_l = \{h_{\pi(s_l+1)}, \cdots, h_{\pi(s_l+n_l)}\}$ and M_m over the set of sub-carriers $\mathscr{H}_m = \{h_{\pi(s_m+1)}, \cdots, h_{\pi(s_m+n_m)}\}$, then for all $l \neq m$, $|h_l| \geq |h_m|$ with $h_l \in \mathscr{H}_l$ and $h_m \in \mathscr{H}_m$, and with $s_l = \sum_{i=1}^{l-1} n_i$.*

This result can simply be interpreted as follows: Π has to be built such that the first Hadamard matrix M_1 is distributed over n_l sub-carriers corresponding to the highest amplitudes $|h_i|$, M_2 over the remaining highest n_l sub-

carriers, and so on. Consider the following example to illustrate the proposition. Let

$$H = \begin{pmatrix} 1 & & & 0 \\ & 0.4 & & \\ & & 0.3 & \\ 0 & & & 0.6 \end{pmatrix} \tag{51}$$

be the channel matrix and

$$M = \begin{pmatrix} 1 & 1 & & 0 \\ 1 & -1 & & \\ & & 1 & 1 \\ 0 & & 1 & -1 \end{pmatrix} \tag{52}$$

be the M-precoding matrix, made of two block matrices M_l with $n_l = 2$. Proposition 6 indicates that the permutation matrix must be such that channel gains are gathered two by two in descending order. This reads

$$\Pi = \begin{pmatrix} 1 & 0 & 0 & 0 \\ 0 & 0 & 1 & 0 \\ 0 & 0 & 0 & 1 \\ 0 & 1 & 0 & 0 \end{pmatrix}. \tag{53}$$

Finally we obtain the following precoding matrix

$$C = \begin{pmatrix} 1 & 1 & 0 & 0 \\ 0 & 0 & 1 & 1 \\ 0 & 0 & 1 & -1 \\ 1 & -1 & 0 & 0 \end{pmatrix}. \tag{54}$$

Note that the same result would be obtained sorting channel gains in ascending order instead of descending order.

The first sub-problem being solved, it remains now to find the optimal set of Hadamard matrices M_l, that is to say find the number k of matrices and their size n_l to maximise the bit-rate. This search is again a combinatorial optimisation problem. In this case the number of solutions is given by the number of partitions of the integer n using as addends integers 1, 2, and all multiples of 4. The generating function of such a number of partitions is

$$\frac{1}{1-x} \frac{1}{1-x^2} \prod_{n=1}^{\infty} \frac{1}{1-x^{4n}} = 1 + x + 2x^2 + 2x^3 + 4x^4 + \cdots = \sum_{n=1}^{\infty} q'(n)x^n. \tag{55}$$

Even if $q'(n)$ is lower than $q(n)$, the search for optimal solution remains intractable in practical systems with high numbers of sub-carriers, and Table 2 gives some values of $q'(n)$.

An heuristic solution is then proposed imposing $n_l = n_m$ for all $\{l,m\} \in [1,k]^2$. In that case, the number of solutions $q''(n)$ is the number of Hadamard matrices with size lower than n. This is the cardinal of the set $\mathcal{K}$ such that $\mathcal{K} = \{n_l | n_l \in \{1,2,4s\}, s \in \mathbb{N} \text{ and } n_l \leq n\}$. The search for the optimal solution within this subset of matrices becomes tractable as the number $q''(n)$ remains low enough. If n_l is well chosen, this heuristic approach, which is suboptimal, performs very close to the optimal solution obtained among the $q(n)$ possible ones [12, 33]. Note that if n is not a multiple of n_l, the remaining sub-carriers are also gathered within one or more matrices of different sizes to not waste these remaining sub-carriers.

3.5 Bit rate maximisation: Examples

In this section, we propose to lead comparative performance evaluation of the introduced adaptive multicarrier systems. In particular, we will assess their capability in terms of bit-rate maximisation under peak-power constraint. For that purpose, we use the power line channel model developed in the context of home network applications [34]. This model defines 9 classes of channel sorted by capacity and built up from measurement campaigns in various PLC environments. The useful channel bandwidth is set to 1.8–87.5 MHz and the power mask expressed in dBm/Hz is given in Figure 2.
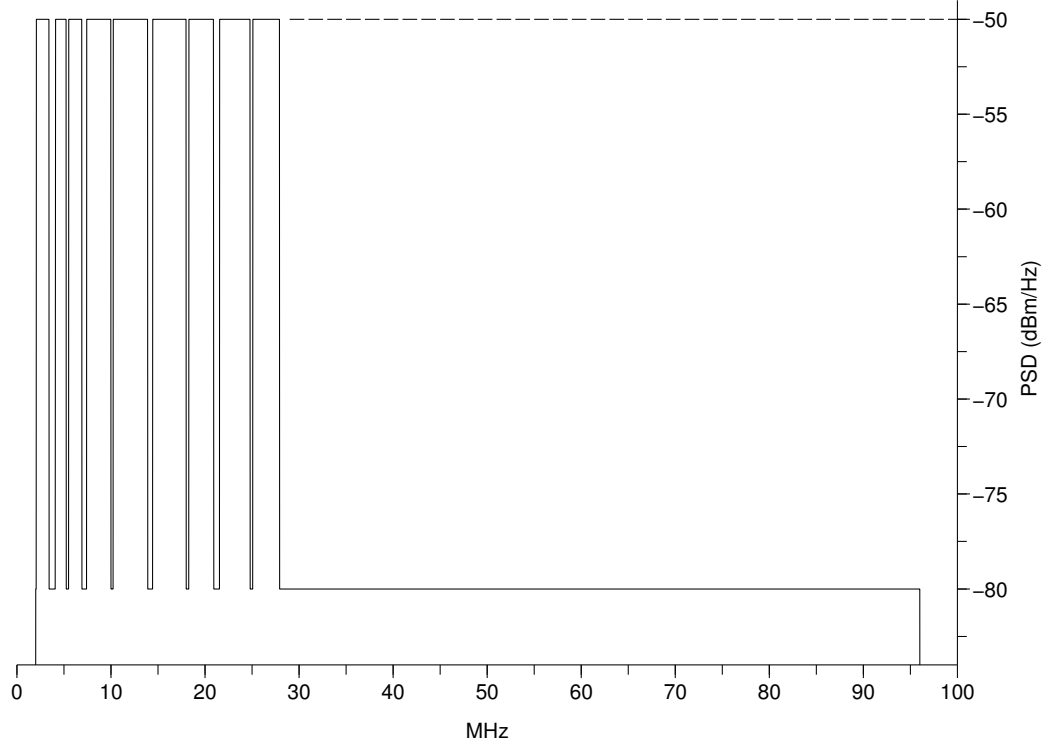
Figure 2: Power mask [36].

Concerning the multicarrier parameters, the sub-carrier spacing and the guard time are compliant with the HPAV ones. An example of the received SNR per sub-carrier is given in Figure 3 for the channel classes 2, 5 and 9. These SNR values reflect the channel transfer function but take also into account the power mask limitation as defined in Figure 2, the coloured background noise and the radio interference noise following the model defined in [35]. In addition, the analog-to-digital conversion noise is also integrated in the SNR values as evident from the SNR saturation floor around 48 dB in the figure. Note that among the 3 chosen classes, class 9 gives the highest SNR values while class 2 corresponds to the worst channel environment. Concerning bit allocation, the maximal bit-rate is set to $r = 10$ with granularity factor $\beta = 1$. In other terms, the utilised modulations are QAM from BPSK to 1024-QAM with all square and rectangular constellations. The SNR-gap γ is chosen to 4 dB corresponding to an SER of 1 % without channel coding. Note that the analog-to-digital conversion noise clip at 48 dB is higher than the needed SNR for 1024-QAM at SER of 1 %. Then, this noise will not limit the maximal achievable bit-rate of the OFDM system.

Using these system and channel parameters, we first propose simulation results in terms of achieved bit-rate under target SER constraint for LP-OFDM using various lengths of precoding sequences. Figure 4 gives the achieved bit-rate versus the precoding sequence length for three examples of channel responses extracted from channel classes 2, 5 and 9. Note that the OFDM performance is obtained for a precoding sequence length equal to unity, while LP-OFDM performance corresponds to other lengths. The depicted curves clearly illustrate the trade-off that should be made about the precoding sequence length to maximise the available power exploitation while minimising the negative impact of the noise power boost due to ZF equalisation. The optimal precoding sequence length is between 12 and 100 which proves that OFDM is not, in fact, the optimal system when discrete modulations are used. This is essentially due to the power loss that occurs with finite order modulations under peak-power constraint in OFDM. In contrast to that,
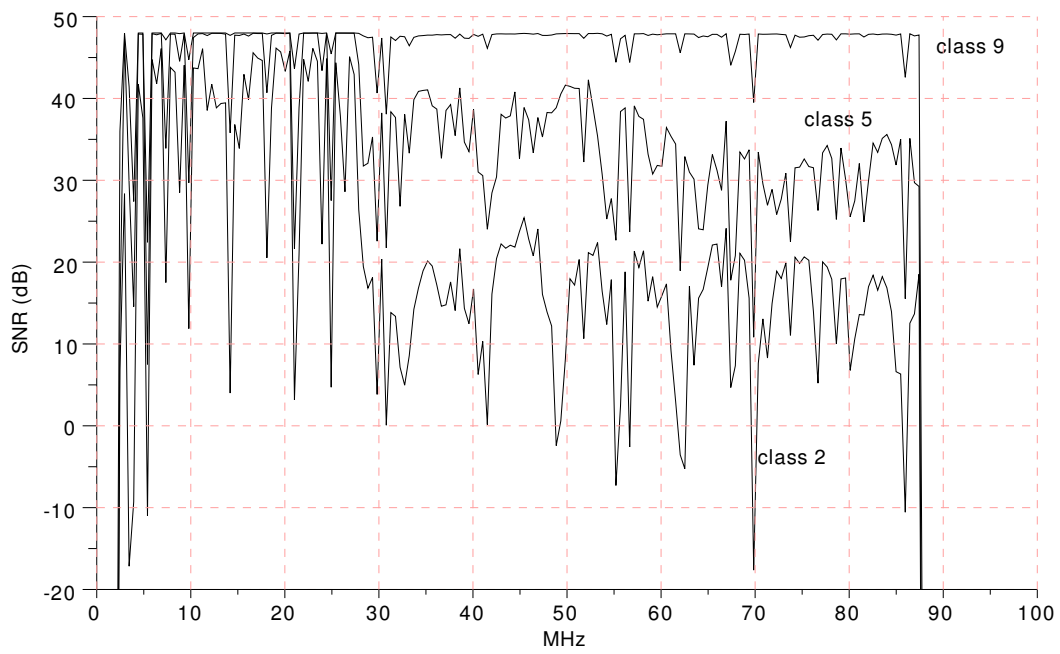
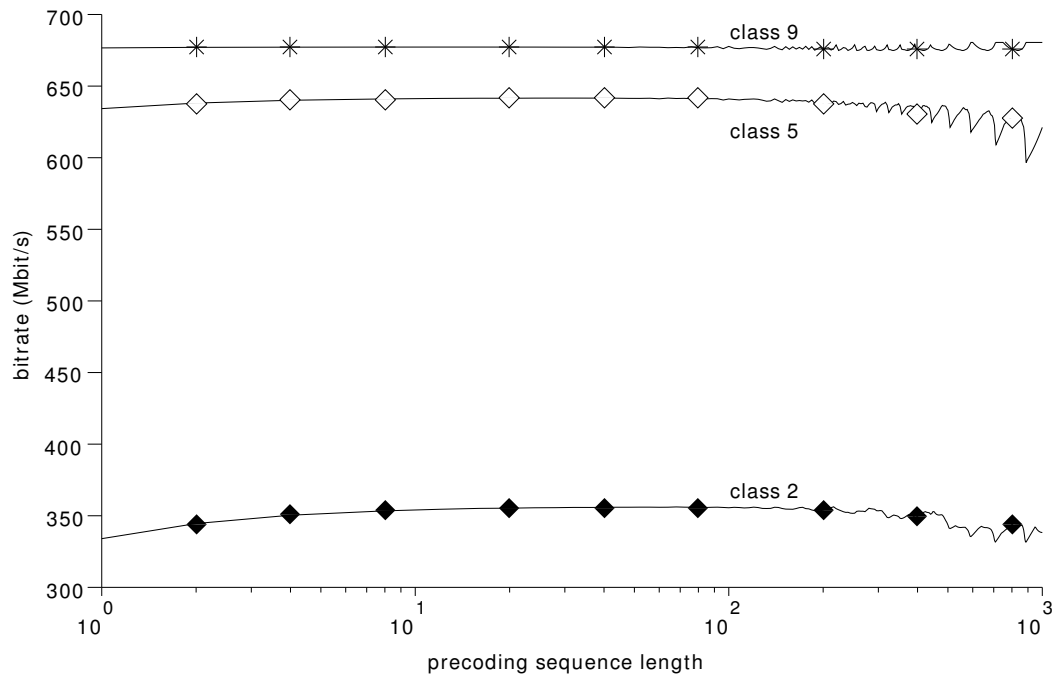Figure 3: SNR per sub-carrier through channel classes 2, 5 and 9.

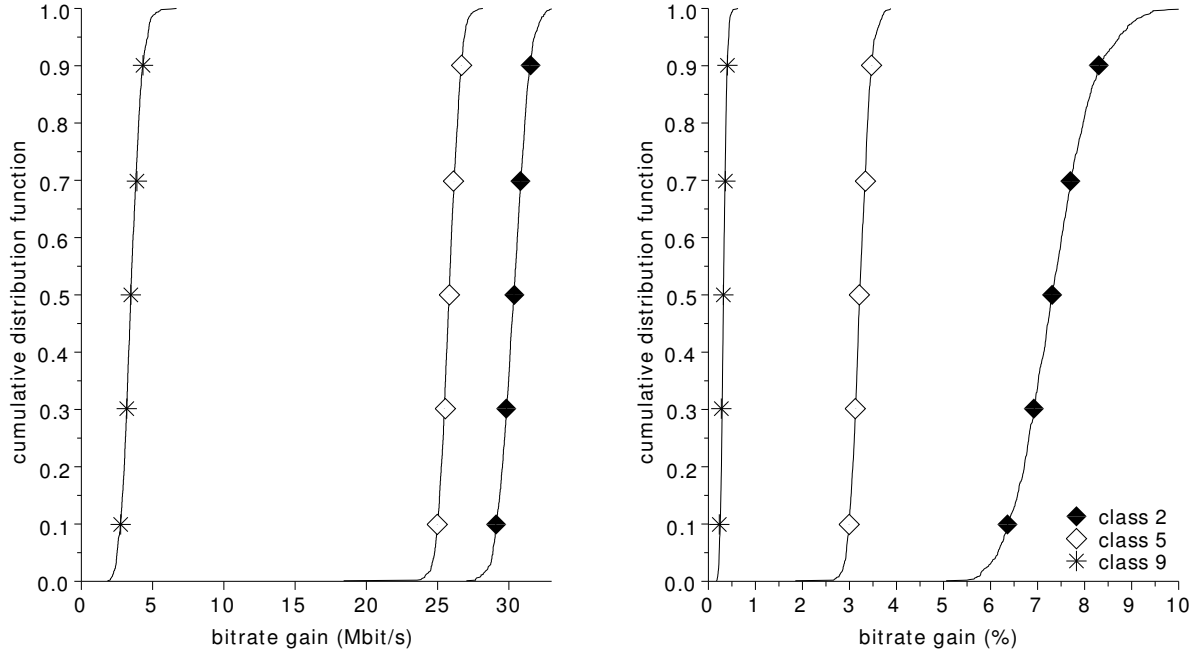Figure 4: Bit-rates versus precoding sequence lengths, $\gamma = 4$ dB.

Figure 5: Cumulative distribution function of the precoding bit-rate gain, $n_l = 32$, $\gamma = 4$ dB.

the power gathering capability of the precoding function can translate into additional bit-rate transmission. However, the bit-rate gain remains moderate and can even be almost null with very good channel conditions, namely class 9. To go further in the analysis, Figure 5 shows the cumulative distribution functions (CDF) of the precoding bit-rate gain in Mbit/s and the relative bit-rate gain in percent of the bit-rate achieved with OFDM. These CDF are obtained fixing $n_l = 32$ and running 1000 trials of channel responses within each classes 2, 5 and 9. The curves tend to show that the bit-rate gain is more significant for poor channel classes than for good channels. This can be understood by the fact that power gathering effects are all the more profitable than SNR values are low. The bit-rate gains in percent remain lower than 10 % but this corresponds in channel classes 2 or 5 to an additional bit-rate of at least 20 Mbit/s compared to OFDM. Considering practical end-device applications, this latter figure is anything but negligible and can in fact be viewed as a new possibility for more high definition TV streaming for example. Note that the bit-rates given in Figure 4 are around 350 Mbit/s for channel class 2, less than 650 Mbit/s for channel class 5, and more than 650 Mbit/s for channel class 9.

Similar simulation results are given in Figure 6 in the case of BER constraint of 1 % instead of SER constraint, again without channel coding. The same precoding sequence length as in previous Figure 5 is used, namely $n_l = 32$. As evident from the CDF curves corresponding to channel class 2, this size of precoding matrix is not a judicious choice since the precoding gain can become negative which means a bit-rate reduction compared to OFDM. As shown in Figure 7, bit-rate gains can be all the time positive if the precoding sequence length is adapted to the channel conditions. In this figure, we give the CDF of the optimal precoding sequence length exhaustively sought among all possible lengths as discussed in Section 3.4. Accordingly, the CDF of the precoding bit-rate gain is plotted considering that the optimal length is used. In average, one can notice that the precoding sizes are lower with good channel conditions than with poor channel conditions, which keeps in line with previous observations and comments. However, the optimal precoding sequence length is not unique within each channel class and should actually be adaptively searched to achieve maximal bit-rate for each channel. As done for the bit-rate and the power, the precoding should be adaptive to yield the highest gains. For complexity reason however, fixed values can reasonably be envisaged. In the proposed example, 32 appears
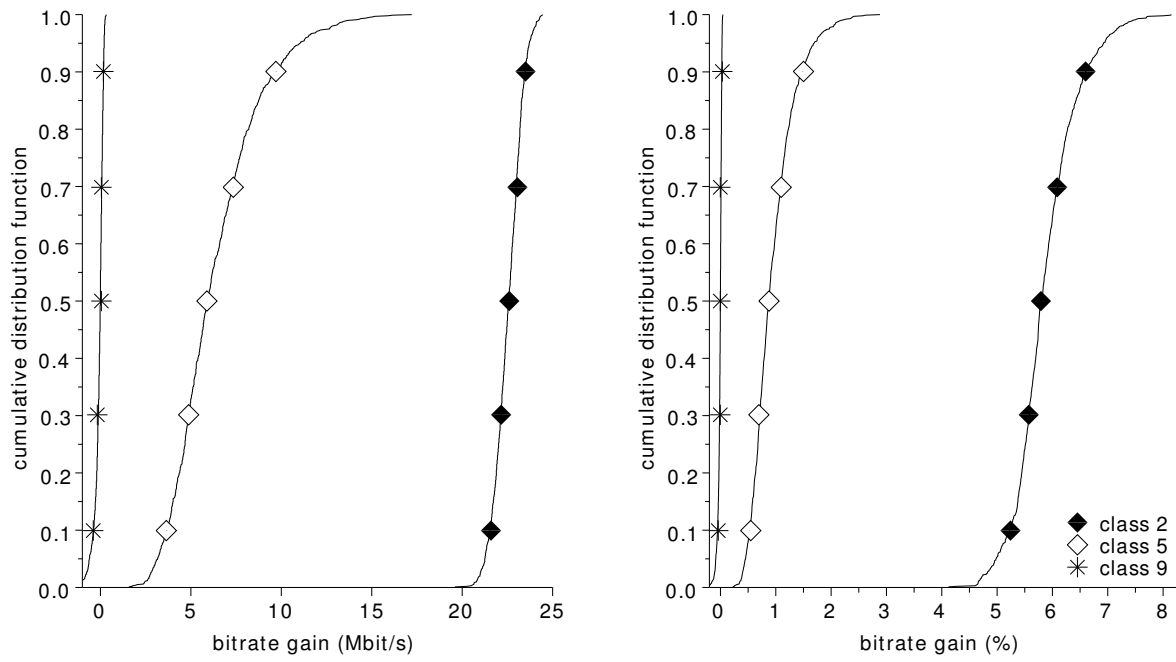
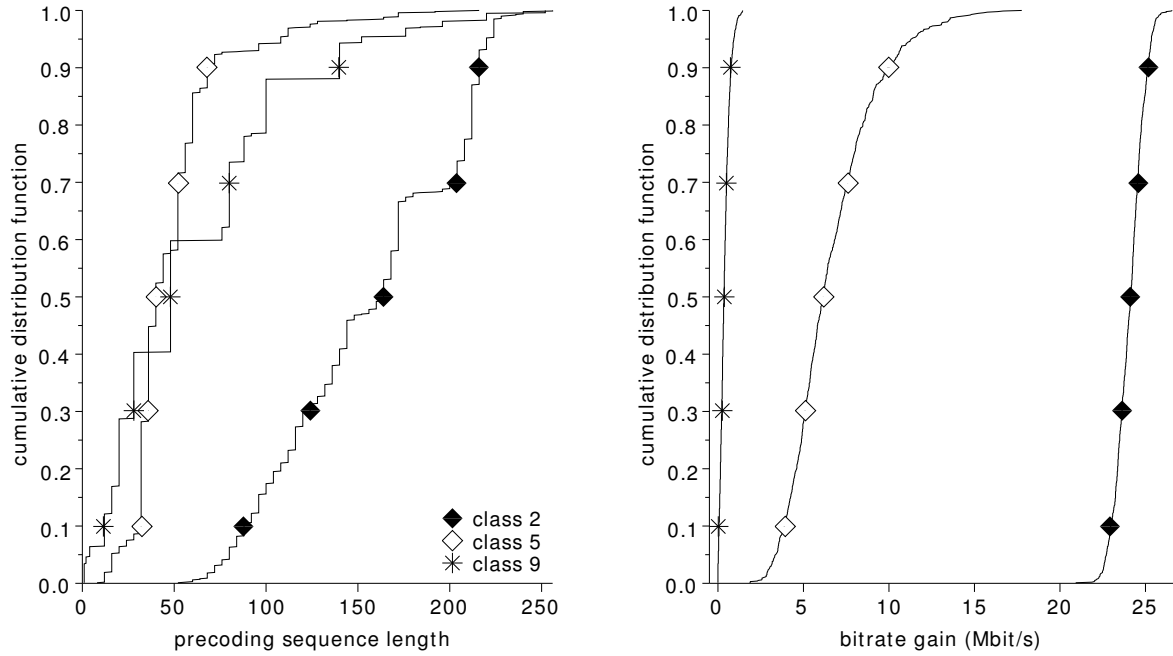Figure 6: Cumulative distribution function of precoding bit-rate gain, $n_l = 32$, BER constraint of 10^{-2}.

Figure 7: Cumulative distribution functions of optimal precoded sequence lengths and of bit-rate gains, BER constraint of 10^{-2}.

as a good trade-off except for channel class 9 that would rather need lower sizes.

Last but not least, it is interesting to compare the bit-rate gain obtained using the MMSE detector instead of the ZF one. Through simulations, it turns out that the MMSE-LP-OFDM system outperforms the ZF-LP-OFDM one, but in a range of less than 0.1 % whatever the precoding sizes. This can be understood by the fact that the design of the permutation matrix Π, given in Proposition 6, leads to very low channel frequency selectivity. Consequently, the MMSE receiver can not efficiently improve the ZF receiver performance and the impact on bit-rates becomes negligible.

4 From time precoding to 2D-precoding extension

In the previous section, we have investigated the resource allocation issue in LP-OFDM systems when the precoding function is applied along the frequency axis as in MC-CDMA systems. It is now interesting to extend the study to the case when precoding is applied in the time domain [11] as in MC-DS-CDMA, and even when applied in both time and frequency domains as firstly proposed for mobile communications in [37].

With precoding in the time domain, the data symbols are spread over n OFDM symbols, instead of n sub-carriers with frequency-wise precoding. The discrete bit-rate r_i on sub-carrier i is straightforwardly derived from Proposition 3 and reads

$$r_i = n \left\lfloor \frac{R_i}{n} \right\rfloor_\beta + \beta \left\lfloor n \frac{2^{R_i/n - \lfloor R_i/n \rfloor_\beta} - 1}{2^\beta - 1} \right\rfloor_1 , \tag{56}$$

with

$$R_i = n \log_2 \left(1 + \frac{|h_i|^2 p}{\gamma \sigma^2} \right) . \tag{57}$$

Note that (57) takes the form of the achievable rate for one sub-carrier of a classical OFDM system without precoding, see (33), simply because the channel fading h_j in (38) is supposed to remain constant over the precoding sequence length. Both systems, OFDM and LP-OFDM, have thus the same achievable rate considering continuous bit-rates. With discrete modulations, the corresponding OFDM bit-rate within sub-carrier i is n times the bit-rate given in (34)

$$r_i = n \left\lfloor \frac{R_i}{n} \right\rfloor_\beta . \tag{58}$$

Comparing (56) and (58), we can conclude that LP-OFDM leads to higher throughput than OFDM if both systems are constrained to use discrete modulations. These results can also be derived with target BER constraint using γ_i instead of γ. The following corollary can then be established.

Corollary 3. *The discrete bit-rate achieved by the time-precoded OFDM system is unconditionally higher that of the non-precoded OFDM system.*

Indeed, the OFDM performance is limited by the granularity of the constellation size, i.e. β. The precoding artificially improves this granularity thanks to its power gathering effect. It can hereby partially compensate for the power loss that occurs with OFDM. More precisely, the discrete bit-rate approaches the continuous bit-rate with increasing n, yet with a residual margin that depends on the continuous value. To evaluate this margin, let us use (56) and (57) to write

$$\frac{R_i}{n} - \frac{\beta}{2^\beta - 1} + \frac{\log \frac{\beta \log 2}{2^\beta - 1} + 1}{\log 2} \leq \lim_{n \to \infty} \frac{r_i}{n} \leq \frac{R_i}{n}, \tag{59}$$

the right-hand equality being obtained when $R_i/(n\beta) \in \mathbb{N}$. Figure 8 shows the discrete bit-rates r_i/n achieved on one sub-carrier in OFDM (58), in LP-OFDM (56) with $n = 4$, and for upper-bound LP-OFDM, i.e. for $n = \infty$. Results are given in reference to the continuous bit-rate case and highlight the evolution of the discrete bit-rates obtained for an increasing continuous bit-rate. Two examples are proposed for $\beta = 1$ and $\beta = 2$. The staircase functions, which are typical of discrete modulation allocation, show that the precoding operation improves the bit-rate granularity regardless of β, whereas the OFDM bit-rate is directed by the value of β. The residual difference between the continuous bit-rate and the upper-bound LP-OFDM bit-rate given by (59) is at most 0.0861 with $\beta = 1$ and 0.3378 with $\beta = 2$.

It is now interesting to evaluate the bit-rate gain introduced by the precoding in time domain. Let q_i be this gain

$$q_i = r_i(\text{LP-OFDM}) - r_i(\text{OFDM}) . \tag{60}$$

The ratio q_i/n is upper-bounded by

$$\lim_{n \to \infty} \frac{q_i}{n} = \frac{\beta}{2^\beta - 1} \left(2^{R/n - \lfloor R/n \rfloor_\beta} - 1 \right) . \tag{61}$$

With the assumption of a uniform distribution of $R/n - \lfloor R/n \rfloor_\beta$ in $[0, \beta)$, the mean value of this upper-bound reads

$$\mathrm{E} \left[\lim_{n \to \infty} \frac{q_i}{n} \right] = \frac{1}{\log 2} - \frac{\beta}{2^\beta - 1} , \tag{62}$$

which is equal to 0.44 with $\beta = 1$ and 0.77 with $\beta = 2$. In other words, this means that a gain of 0.44 bits per sub-carrier can be expected from the use a precoding function if uncoded QAM modulations are considered in the transmission scheme.

The bit-rate gain introduced by the precoding is upper-bounded and, in average, increases with β. To reach the upper-bound, large matrix sizes should be used. A strong drawback of this is that the data are decoded at the receiver once all the OFDM symbols linked by the precoding matrix are received. This can introduces very large delays for the signal decoding in the receiver. A possible solution is then to fold up a part of the precoding matrix in the frequency domain, thus leading to so-called 2D precoding. Through this approach, the system can benefit from time-domain precoding advantages without suffering from too long decoding delay, and, in the same way can take advantage of the frequency-domain precoding gain while limiting the effects of frequency selectivity. For that purpose, the 2D-precoding size in time and frequency has to be judiciously chosen through a trade off between:
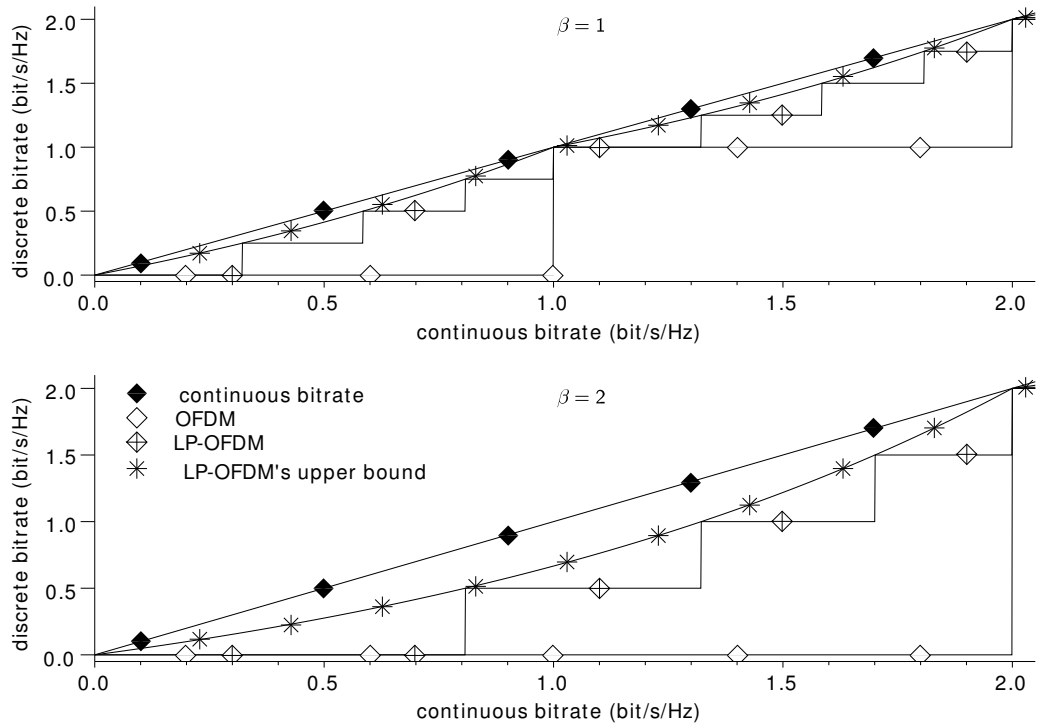
Figure 8: Discrete bit-rate r_i/n versus continuous bit-rate with $n \in \{1, 4, \infty\}$ and $\beta \in \{1, 2\}$.

- bit-rate gain and delay, for time-domain precoding length,

- bit-rate gain and frequency distortion, for frequency-domain precoding length.

The optimal choice is thus to use precoding sequences as long as possible in time and frequency while limiting the frequency distortion as much as possible and getting acceptable delays. In practice, multiple configurations exist that yield discrete bit-rates higher than 99.5 % of the OFDM continuous bit-rate [13]. 2D-precoding is thus an efficient solution to achieve almost optimal bit-rates in multicarrier systems.

5 Multicast scenarios

Multicasting is a technique that allows data, including packet form, to be simultaneously transmitted to a selected set of destinations [38]. In other terms, the same data are transmitted to several receivers at the same time. Multicasting is a more efficient method of supporting group communications than unicasting or broadcasting, as it allows transmission to multiple destinations using fewer network resource [39]. It is particularly useful for high data rate multimedia services due to its ability to save the network resource. Contrary to unicasting, the multicast service does not repeat multiple time the same transmission and, contrary to broadcasting, the multicast data are addressed to known receivers. With the knowledge of the receivers, the source, i.e. the transmitter, can evaluates the channel conditions of each link. Based on the channel estimation and on the quality of service requirements, the source has the capability to adapt the multicast bit-rate to the channel conditions.

5.1 Resource allocation

As in Section 2.1.1, we will assume throughout this section that the multicarrier system is well adapted to the channel and perfectly synchronised in time and frequency. All CSI of the multicast environment are supposed to be known at both transmitter and receiver sides. We consider n sub-carriers and u receivers. The signal received by receiver j then writes

$$Y_j = H_j P^{1/2} X + N, \tag{63}$$

where H_j conveys the channel coefficients for the communication link created between the transmitter and the jth receiver. The resulting OFDM multicast discrete bit-rate then reads

$$r = u \sum_{i=1}^{n} \min_{j \in [1,u]} \left\lfloor \log_2 \left(1 + \frac{p}{\gamma \sigma^2} |h_{i,j}|^2 \right) \right\rfloor_\beta, \tag{64}$$

with $h_{i,j}$ the updated notation for channel gains h_i taking into account receiver index j. In the latter equation, it can be noticed that the multicast bit-rate is governed by the worst channel conditions among the links defined by the multicast environment. Hence, the allocation can be computed using equivalent channel

$$|\tilde{h}_i| = \min_{j \in [1,u]} |h_{i,j}| \tag{65}$$

and the OFDM multicast discrete bit-rate becomes

$$r = \sum_{i=1}^{n} u \lfloor r_i \rfloor = u \sum_{i=1}^{n} \left\lfloor \log_2 \left(1 + \frac{|\tilde{h}_i|^2 p}{\gamma \sigma^2} \right) \right\rfloor_\beta. \tag{66}$$

This bit-rate is also given by (34) using the multicast equivalent channel and without taking into account the multiplicative factor u. Through independent and identically distributed Rayleigh fading channels, and using order statistics [40], we have that

$$\lim_{u \to \infty} u r_i = \frac{p}{\gamma \sigma^2 \log 2} \tag{67}$$

for all i. Consequently, it comes that

$$\lim_{u \to \infty} r = 0. \tag{68}$$

Hence, the drawback of such a multicast method based on the poorest channel conditions, is that it can lead to dramatic degradation of the bit-rate when the number of receivers increases. The so-called multirate multicast approach is a method that overcomes this drawback. The basic idea is to order the multicast data into layers so that each receiver can decode any combination of the layers depending on its link quality. This method is well adapted to OFDM transmission [41] and can be extended to LP-OFDM signal [26]. In the sequel, we will however demonstrate that the precoding function already brings bit-rate improvement in the unirate multicast case.

5.1.1 Linear precoding and multicast

Let us first consider non sparse precoding matrices applied in the frequency domain and ZF reception. The discrete multicast bit-rate is then derived from Proposition 3 using $\tilde{H}$ in (38) instead of H [42, 33]. As mentioned before in the OFDM case, the discrete bit-rate also converges to 0 when the number of receivers goes to infinity, regardless of the precoding sequence length. Note that with sparse precoding matrices, the method presented Section 3.4 can be applied, however leading again to null bit-rates for an infinite number of receivers. We may then ask whether we can expect better performance from the unirate multicast approach.

For that purpose, it is interesting to express the continuous multicast bit-rate as the minimal continuous precoding bit-rate. In this case, the computation of the bit-rate takes into account the diversity of the receivers [43]. Using (38) yields

$$R = u \min_{j \in [1,u]} n \log_2 \left(1 + \frac{1}{\gamma} \frac{n}{\sum_{i=1}^{n} \frac{1}{|h_{i,j}|^2}} \frac{p}{\sigma^2} \right),$$

(69)

which can be lower bounded as

$$R \geq un \log_2 \left(1 + \frac{1}{\gamma} \frac{n}{\sum_{i=1}^{n} \frac{1}{|\tilde{h}_i|^2}} \frac{p}{\sigma^2} \right)$$

(70)

because $|\tilde{h}_i| \leq |h_{i,j}|$ for all $i \in [1,n]$ and all $j \in [1,u]$. It can be verified that this inequality remains valid considering discrete bit-rate. The latter is computed using (69) and Proposition 3 under SNR-gap constraint or Proposition 5 under BER constraint. Interestingly, it appears that the multicast continuous bit-rate can be improved employing precoding principles, whereas we have shown in 2.4 that precoding always reduces the unicast continuous bit-rate. With a large number of receivers, we understand that the multicast bit-rate will be degraded, yet keeping the advantage over the non-precoded system.

As in Section 3, it remains to find the optimal matrix C in the case of sparse matrices.

5.1.2 Practical solution

The problem is similar to the one encountered in Section 3.4. It is then solved in the same way using the heuristic solution for which the equivalent channel is used for the design of the permutation matrix Π. We can then rapidly state the following result.

Corollary 4. *The multicast discrete bit-rate is*

$$r = u \sum_{l=1}^{k} n_l \left\lfloor \frac{R_l}{un_l} \right\rfloor_\beta + u\beta \left\lfloor n_l \frac{2^{R_l/un_l - \lfloor R_l/un_l \rfloor_\beta} - 1}{2^\beta - 1} \right\rfloor_1,$$

with

$$R_l = u \min_{j \in [1,u]} n_l \log_2 \left(1 + \frac{1}{\gamma} \frac{n_l}{\sum_{i=1}^{n_l} \frac{1}{|h_{\pi(n_1 + \cdots + n_{i-1} + i),j}|^2}} \frac{p}{\sigma^2} \right).$$

This result can also be extended in the case of BER constraint, and Proposition 5 should be used instead of Proposition 3.
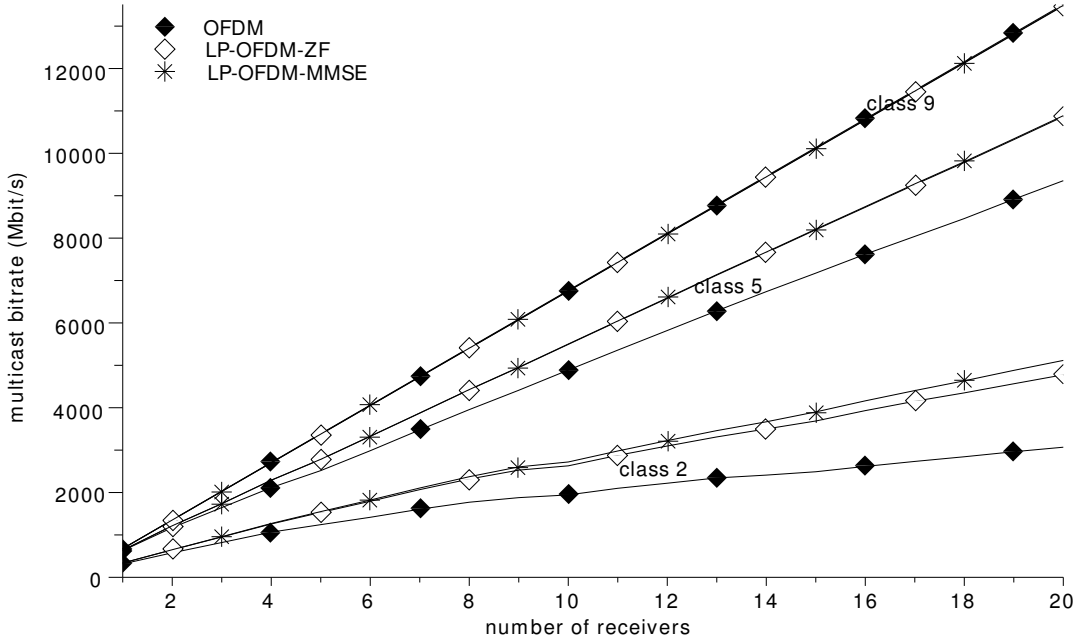
Figure 9: Multicast bit-rates versus number of receivers, $n_l = 64$, $\gamma = 4$ dB.

5.2 Bit rate maximisation: Examples

The multicast performance gains obtained with the precoding component are evaluated through the channel model presented in Section 3.5. The variations of the discrete multicast bit-rate versus the precoding sequence lengths are similar to those encountered in the case of unicast shown in Figure 4. We consequently choose the spreading length $n_l = 64$ hereafter.

It is first interesting to observe the variation of the total multicast bit-rate when the number of receivers increases as depicted in Figure 9. In this figure, we compare the bit-rates obtained for 3 different classes of channels and carrying out OFDM, LP-OFDM with ZF and MMSE detectors. It can be viewed that the gain provided by the precoding function is much more visible for the most severe channels than for the less ones. As in the unicast scenario, the precoding does not improve significantly the bit-rate in very good channels as evident from the results of class 9. For class 2 and 5, one can note that the relative gain is quite independent of the number of receivers and that the absolute gain depends linearly of this number of receivers. This result remains true if the number of receivers is not too high. Considering a very high number of receivers, the bit-rate would saturate and for even more receivers it would decrease and tend to zero. The last important remark is that the additional gain provided by the MMSE detector over the ZF detector is very reduced. The ZF detector can thus be viewed as the best trade-off between performance and complexity.

In Figure 10, we give the CDF of the bit-rate gains obtained with LP-OFDM through various channel realisations: each link is chosen within one of the 9 channel classes following the channel percentage of classes [34]. Precoding lengths are set to 4, 8 and 64, and $u = 5$ receivers are used in the multicast network. On the left side of the figure, the gains are computed with reference to OFDM ; on the right side, comparison is made between MMSE and ZF detectors. It clearly appears that LP-OFDM outperforms OFDM with bit-rate gains higher than 100 Mbit/s in more than 90% of the cases. The highest gain is obtained with $n_l = 64$, that is when the sub-carrier gathering effect of the precoding component is already high. As far as the MMSE detector is concerned, one can notice that the gain over the ZF detector remains much more moderated. For example, MMSE brings less than 10 Mbit/s gain with a probability of around 50%.
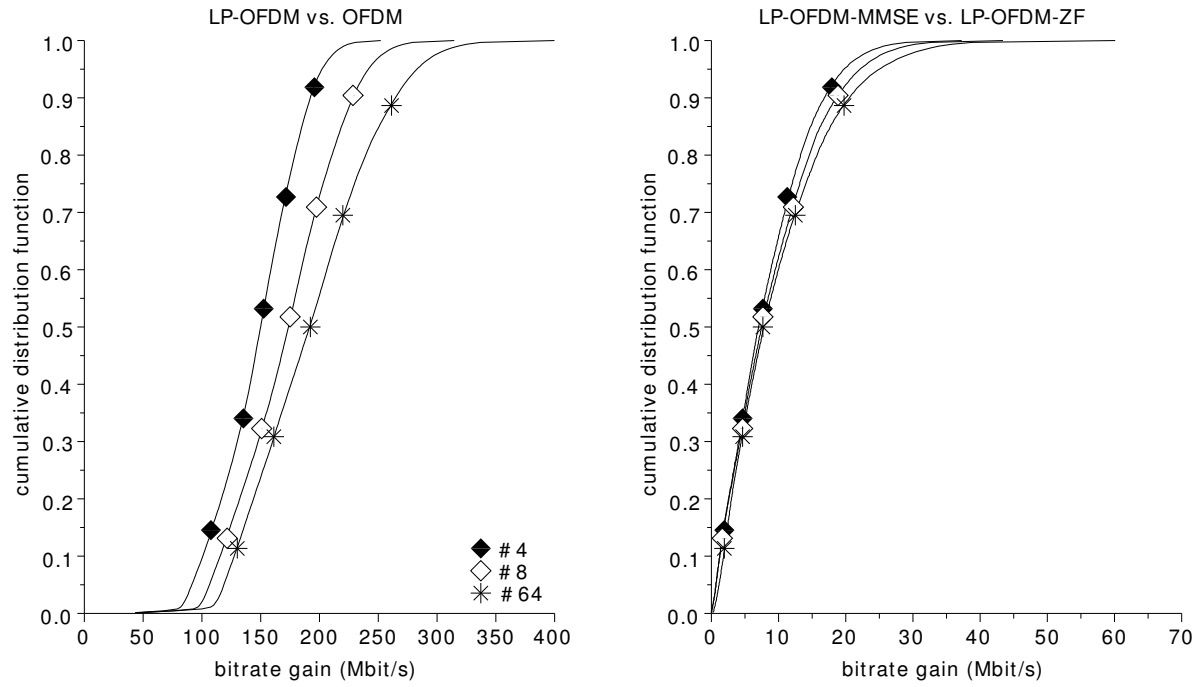
Figure 10: Cumulative distribution function of bit-rate gains of LP-OFDM-ZF compared to OFDM and LP-OFDM-MMSE compared to LP-OFDM-ZF, $u = 5$, $\gamma = 4$ dB.

In addition, the comparative performance between MMSE and ZF has very weak dependence on the precoding length.

Finally, these results confirm that LP-OFDM is profitable in a multicast context compared to OFDM and that most of the expected gain is obtained using a simple ZF detector.

6 Conclusion

In this chapter we have reviewed the principle and the major results of adaptive precoded OFDM communication system. Simple precoding added to conventional OFDM system leads to bit-rate improvement in point to point communication as well as in multicast power line environment. These bit-rate gains up to 30 Mbit/s, and up to 10% of the OFDM bit-rates, allow transmission of more high definition TV flows in home network. The simple solution for bit-rate increase based one Hadamard matrices can benefit from fast Hadamard transform for efficient realisation and can be combined with enhanced OFDM systems.

Acknowledgements

References

[1] S. Weinstein, "The history of orthogonal frequency-division multiplexing," *IEEE Communications Magazine*, vol. 47, no. 11, pp. 26–35, Nov. 2009.

[2] M. Simon, J. Omura, R. Scholtz, and B. Levitt, *Spread spectrum communications handbook*. McGraw-Hill, 2001.

[3] S. Hara and R. Prasad, "Overview of multicarrier CDMA," *IEEE Communications Magazine*, pp. 126–133, Dec. 1997.

[4] M. Debbah, W. Hachem, P. Loubaton, and M. de Courville, "MMSE analysis of certain large isometric random precoded systems," *IEEE Transactions on Information Theory*, vol. 49, no. 5, pp. 1293–1311, May 2003.

[5] S. Mallier, F. Nouvel, J.-Y. Baudais, D. Gardan, and A. Zeddam, "Multicarrier CDMA over lines — comparison of performances with the ADSL system," in *IEEE International Workshop on Electronic Design, Test and Applications*, Jan. 2002, pp. 450–452.

[6] O. Isson and J-M. Brossier et D. Mestdagh, "Multi-carrier bit-rate improvement by carrier merging," *Electronics Letters*, vol. 38, no. 19, pp. 1134–1135, Sep. 2002.

[7] M. Crussière, J.-Y. Baudais, and J.-F. Hélard, "Robust and high-bit rate communications over PLC channels: A bit-loading multi-carrier spread-spectrum solution," in *International Symposium on Power-Line Communications and Its Applications*, Vancouver, Canada, Apr. 2005, pp. 37–41.

[8] ——, "New loading algorithms for adaptive SS-MC-MA systems over power line channels: Comparisons with DMT," in *International Workshop on Multi-Carrier Spread Spectrum*, Oberpfaffenhofen, Germany, 14–16 Sep. 2005, pp. 327–336.

[9] M. Raug, T. Zheng, M. Tucci, and S. Barmada, "On the time invariance of PLC channels in complex power networks," in *IEEE International Symposium on Power Line Communications and Its Applications*, Copacabana Rio de Janeiro, Brazil, Mar. 2010, pp. 56–61.

[10] K.-H. Kim, H.-B. Lee, Y.-H. Kim, and S.-C. Kim, "Channel adaptation for time-varying powerline channel and noise synchronized with AC cycle," in *IEEE International Symposium on Power Line Communications and Its Applications*, Apr. 2009, pp. 250–254.

[11] M. Crussière, J.-Y. Baudais, and J.-F. Hélard, "Improved throughtput over wirelines with adaptive MC-DS-CDMA," in *International Symposium on Spread Spectrum Techniques and Applications*, Manaus-Amazomn, Brazil, 28–31 Aug. 2006, pp. 143–147.

[12] ——, "Adaptive linear precoded DMT as an efficient resource allocation scheme for power-line communications," in *IEEE Global Communications Conference*, ser. 5, no. 1, San Francisco, California, USA, Dec. 2006.

[13] J.-Y. Baudais and M. Crussière, "Resource allocation with adaptive spread spectrum OFDM using 2D spreading for power line communications," *EURASIP Journal on Advances in Signal Processing*, vol. 2007, pp. 1–13, 2007, special issue on Advanced Signal Processing and Computational Intelligence Techniques for Power Line Communications.

[14] S. Kaiser, "OFDM code-division multiplexing in fading channels," *IEEE Transactions on Communications*, vol. 50, no. 8, pp. 1266–1273, Aug. 2002.

[15] S. Verdú, *Multiuser detection*. New York: Cambridge University Press, 1998.

[16] I.S. Gradshteyn and I.M. Ryzhik, *Table of Integrals, Series, and Products*, 7th ed. USA: Elsevier Academic Press publications, 2007.

[17] M. Crussière, J.-Y. Baudais, and J.-F. Hélard, "Adaptive spread spectrum multicarrier multiple access over wirelines," *IEEE Journal on Selected Areas in Communications*, vol. 24, no. 7, pp. 1377–1388, Jul. 2006, special issue on Power Line Communications.

[18] A. S. Hedayat, N. J. A. Sloane, and John Stufken, *Orthogonal Arrays: Theory and Applications*. Springer-Verlag, New York, 1999, ch. 7.

[19] TR 102 494, *Powerline Telecommunications (PLT) Technical requirements for In-House PLC modems*, ETSI, Jun. 2005.

[20] A.J. Goldsmith and S.-G. Chua, "Adaptive coded modulation for fading channels," *IEEE Transactions on Communications*, vol. 45, no. 5, pp. 595–602, May 1998.

[21] D.P. Palomar, J.M. Cioffi, and M.A. Lagunas, "Joint Tx-Rx beamforming design for multicarrier MIMO channels: a unified framework for convex optimization," *IEEE Transactions on Signal Processing*, vol. 51, no. 9, pp. 2381–2401, Sep. 2003.

[22] J.M. Cioffi, "A multicarrier primer," ANSI T1E1.4/91–157, Committee contribution, Tech. Rep., Nov. 1991.

[23] A. Maiga, J.-Y. Baudais, and J.-F. Hélard, "An efficient channel condition aware proportional fairness ressource allocation for powerline communications," in *International Conference on Telecommunications*, Marrakech, Morocco, 25–27 May 2009, pp. 286–291.

[24] D.P. Palomar and J.R. Fonollosa, "Practical algorithms for a family of waterfilling solutions," *IEEE Transactions on Signal Processing*, vol. 53, no. 2, pp. 686–695, Feb. 2005.

[25] K. Fazel and S. Kaiser, *Multi-carrier and spread spectrum techniques*. The Atrium, Southern Gate, Chichester,West Sussex, England: John Wiley & Sons Ltd, 2003.

[26] A. Maiga, J.-Y. Baudais, and J.-F. Hélard, "Bit rate optimization with MMSE detector for multicast LP-OFDM systems," *Journal of Electrical and Computer Engineering*, vol. 2012, pp. 1–12, 2012.

[27] N. Papandreou and T. Antonakopoulos, "Bit and power allocation in constrained multicarrier systems: The single-user case," *EURASIP Journal on Applied Signal Processing*, vol. 2008, pp. 1–14, 2008.

[28] F.S. Muhammad, J.-Y. Baudais, and J.-F. Hélard, "Rate maximization loading algorithm for LP-OFDM systems with imperfect CSI," in *IEEE Personal, Indoor and Mobile Radio Communications Symposium*, Tokyo, Japan, 13–16 Sep. 2009, pp. 1–5.

[29] ——, "Bit rate maximization for LP-OFDM with noisy channel estimation," in *3rd International Conference on Signal Processing and Communication Systems*, Omaha, Nebraska, USA, 28–30 Sep. 2009, pp. 1–6.

[30] S.T. Chung and A.J. Goldsmith, "Degrees of freedom in adaptive modulation: A unified view," *IEEE Transactions on Communications*, vol. 49, no. 9, pp. 1561–1571, Sep. 2001.

[31] A. Maiga, J.-Y. Baudais, and J.-F. Hélard, "Very high bit rate power line communications for home networks," in *IEEE International Symposium on Power Line Communications and Its Applications*, Dresden, Germany, Mar. 2009, pp. 313–318.

[32] J.-Y. Baudais, F.S. Muhammad, and J.-F. Hélard, "Robustness maximization of parallel multichannel systems," *Journal of Electrical and Computer Engineering*, vol. 2012, pp. 1–16, 2012.

[33] A. Maiga, J.-Y. Baudais, and J.-F. Hélard, "Increase in multicast OFDM data rate in PLC network using adaptive LP-OFDM," in *2nd International Conference on Adaptive Science and Technology (ICAST)*. Accra, Ghana: IEEE, 14–16 Dec. 2009, pp. 384–389.

[34] M. Tlich, A. Zeddam, F. Moulin, and F. Gauthier, "Indoor power-line communications channel characterization up to 100 MHz–Part I: One-parameter deterministic model," *IEEE Transactions on Power Delivery*, vol. 23, no. 3, pp. 1392–1401, Jul. 2008.

[35] W.Y. Chen, *Home Network Basis: Transmission Environments and Wired/Wireless Protocols*. Prentice Hall PTR, 2004.

[36] P. Pagani, R. Razafferson, A. Zeddam, B. Praho, M. Tlich, J.-Y. Baudais, A. Maiga, O. Isson, G. Mijic, K. Kriznar, and S. Drakul, "Electromagnetic compatibility for power line communications. Regulatory issues and counter-measures," in *IEEE Personal, Indoor and Mobile Radio Communications Symposium*, Istanbul, Turkey, Sep. 2010, pp. 1–6.

[37] A. Persson, T. Ottosson, and E. Strom, "Time-frequency localized CDMA for downlink multi-carrier systems," in *International Symposium on Spread Spectrum Techniques and Applications*, vol. 1, Sun City, South Africa, Sep. 2002, pp. 118–122.

[38] ATIS-0100523.2011, *ATIS Telecom Glossary*, Alliance for Telecommunications Industry Solutions, Washington, DC, 2011.

[39] U. Varshney, "Multicast over wireless networks," *Communications of the ACM*, vol. 45, no. 12, pp. 31–37, Dec. 2002.

[40] H.A. David and H.N. Nagaraja, *Order statistics*, 3rd ed., ser. Probability and statistics. Wiley-Interscience, 2003.

[41] C. Suh and J. Mo, "Resource allocation for multicast services in multicarrier wireless communications," in *25th IEEE International Conference on Computer Communications.*, Barcelona, Catalunya, Spain, Apr. 2006, pp. 1–12.

[42] A. Maiga, J.-Y. Baudais, and J.-F. Hélard, "Bit rate maximization for multicast LP-OFDM systems in PLC context," in *Third Workshop on Power Line Communications*, Udine, Italy, Oct. 2009, pp. 93–95.

[43] ——, "Subcarrier, bit and time slot allocation for multicast precoded OFDM systems," in *IEEE International Conference on Communications*, Cape Town, South Africa, 23–27 May 2010, pp. 1–6.